Performance of Alkali-Activated Concrete using Municipal-Waste Incinerator Bottom Ash as a Partial Replacement of Precursor at Elevated Temperatures

By

Muhammad Muneeb Nawaz

(Registration No: 00000360466)

Department of Structural Engineering

NUST Institute of Civil Engineering

School of Civil and Environmental Engineering

National University of Sciences & Technology (NUST)

Islamabad, Pakistan

(2025)

Performance of Alkali-Activated Concrete using Municipal-waste Incinerator Bottom Ash as a Partial Replacement of Precursor at Elevated Temperatures

By

Muhammad Muneeb Nawaz

(Registration No: 00000360466)

A thesis submitted to the National University of Sciences and Technology, Islamabad,

in partial fulfillment of the requirements for the degree of

Master of Science in Structural Engineering

Supervisor: Dr. Junaid Ahmad

Co-Supervisor: Dr. Hammad Anis Khan

School of Civil and Environmental Engineering

National University of Sciences & Technology (NUST)

Islamabad, Pakistan

(2025)

THESIS ACCEPTANCE CERTIFICATE

It is certified that Mr. Muhammad Muneeb Nawaz, Registration No. 00000360466, of MS Structural Engineering of batch 2021 at NUST Institute of Civil Engineering (NICE) has completed his thesis work and submitted final copy which was evaluated and found to be complete in all respects as per policy of NUST Statutes/Regulations, is free of plagiarism, errors, and mistakes and is accepted as partial fulfillment for the award of MS degree. It is further certified that necessary amendments as pointed out by GEC members of the scholar have also been incorporated in the said thesis.

Signature: _____

Supervisor: Dr. Junaid Ahmad

Date: _____14.02.2025_____

Signature: _____

HoD Structural Engineering
NUST Institute of Civil Engineering
School of Civil & Environmental Engineering
National University of Sciences and Technology

Head of Department: Dr. Muhammad Usman

Date: _____14-2-25_____

Signature: _____

Associate Dean: Dr. S. Muhammad Jamil

Date: 17.2.2025

Signature: _____

Principal & Dean (SCEE-NICE): Prof. Dr. Muhammad Irfan

Date: _____17 FEB 2025_____

PROF DR MUHAMMAD IRFAN
Principal & Dean
SCEE, NUST

National University of Sciences and Technology

MASTER'S THESIS WORK

We hereby recommend that the dissertation prepared under our Supervision by: Muhammad Muneeb Nawaz, Regn No. 00000360466

Titled: "Performance of Alkali-Activated Concrete using Municipal-waste Incinerator Bottom Ash as a Partial Replacement of Precursor at Elevated Temperatures" be accepted in partial fulfillment of the requirements for the award of degree with ___A___ Grade.

Examination Committee Members

1. Name: Dr. Hammad Anis Khan   Signature: _____

2. Name: Dr. Muhammad Usman   Signature: _____

3. Name: Dr. Muhammad Imran   Signature: _____

Supervisor's name: Dr. Junaid Ahmad   Signature: _____

HoD Structural Engineering
NUST Institute of Civil Engineering
School of Civil & Environmental Engineering
National University of Sciences and Technology

__Head of Department__

(Associate Dean)
Dr. S. Muhammad Jamil
Associate Dean
NICE, SCEE, NUST

COUNTERSIGNED

Date: __11 FEB 2025__

Principal & Dean SCEE
PROF DR MUHAMMAD IRFAN
Principal & Dean
SCEE, NUST

Certificate of Approval

This is to certify that the research work presented in this thesis, entitled "Performance of Alkali-Activated Concrete using Municipal-waste Incinerator Bottom Ash as a Partial Replacement of Precursor at Elevated Temperatures" was conducted by Mr. **Muhammad Muneeb Nawaz** under the supervision of Dr. Junaid Ahmad.

No part of this thesis has been submitted anywhere else for any other degree. This thesis is submitted to the National University of Sciences and Technology (NUST) in partial fulfillment of the requirements for the degree of Master of Science in field of Structural Engineering from NUST institute of Civil Engineering (NICE), School of Civil and Environmental Engineering (SCEE), NUST

Student Name: Muhammad Muneeb Nawaz   Signature: _____

Examination Committee:

a) GEC Member 1: Dr. Muhammad Usman   Signature _____
    Associate Professor (SCEE, NUST)

b) GEC Member 2: Dr. Muhammad Imran   Signature _____
    Assistant Professor (SCEE, NUST)

Co-Supervisor Name: Dr. Hammad Anis Khan   Signature: _____

Supervisor Name: Dr. Junaid Ahmad   Signature: _____

Name of HOD: Dr. Muhammad Usman   Signature: _____
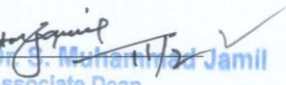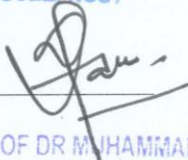   HoD Structural Engineering
                                                     NUST Institute of Civil Engineering
                                                     School of Civil & Environmental Engineering
                                                     National University of Sciences and Technology

Name of Associate Dean: Dr. S. Muhammad Jamil   Signature: _____
                                                     Dr. S. Muhammad Jamil
                                                     Associate Dean
                                                     NICE, SCEE, NUST

Name of Principal & Dean: Prof. Dr. Muhammad Irfan   Signature: _____
                                                     PROF DR MUHAMMAD IRFAN
                                                     Principal & Dean
                                                     SCEE, NUST

AUTHOR'S DECLARATION

I Muhammad Muneeb Nawaz hereby state that my MS thesis titled "Performance of Alkali-Activated Concrete using Municipal-waste Incinerator Bottom Ash as a Partial Replacement of Precursor at Elevated Temperatures" is my own work and has not been submitted previously by me for taking any degree from National University of Sciences and Technology, Islamabad or anywhere else in the country/ world.

At any time if my statement is found to be incorrect even after I graduate, the university has the right to withdraw my MS degree.

Name of Student: Muhammad Muneeb Nawaz

Date: 13th January 2025

DEDICATION

This thesis is humbly dedicated to my dear parents and family for whose immeasurable support, sacrifice, prayers, and faith I have produced. They have always considered my future, made numerous sacrifices, and committed that I should maintain good moral character. I also dedicate this to all my teachers, those who have imparted knowledge and provided the foundation and motivation throughout my learning process.

ACKNOWLEDGEMENTS

TABLE OF CONTENTS

LIST OF TABLES

LIST OF FIGURES

Page No.

LIST OF SYMBOLS, ABBREVIATIONS AND ACRONYMS

AA   alkaline activator

AAC   Alkali-activated concrete

AAMs   Alkali-activated materials

EDS   Energy-dispersive X-ray spectroscopy

FTIR   Fourier Transform Infrared Spectroscopy

FA   Fly ash

GGBFS   Ground granulated blast furnace slag

MIBA   Municipal-waste incinerator bottom ashes

SP   Superplasticizer

SEM   Scanning electron microscopy

TGA   Thermogravimetric Analysis

XRD   X-ray diffraction

XRF   X-ray fluorescence

C-S-H   Calcium silicate hydrate

N-A-S-H   Sodium aluminosilicate hydrate

ABSTRACT

Cement production is one of the world's biggest sources of CO_2 emissions, thus the development of green options like the Alkali-Activated Concrete (AAC). Recently, MIBA is considered as more environmentally friendly material to be used in concrete pavement, but the effects of MIBA on the mechanical and thermal performance of AAC, still have been poorly investigated. That is why the purpose of this study is to assess the applicability of MIBA for partial replacement of FA in AAC while considering the sustainability performance. In this work, MIBA was processed and then analyzed by X-Ray Fluorescence (XRF), X-Ray Diffraction (XRD), Scanning Electron Microscopy (SEM) and Thermogravimetric Analysis (TGA). Concrete samples were prepared by replacing FA with 5–20% MIBA by weight, activated using a 12M sodium hydroxide (NaOH) and sodium silicate (Na_2SiO_3) solution in a 1:2 ratio. The samples were then left to cure at 60°C for 72 hours and then at ambient temperature for 28 days. Compression test was conducted in addition to SEM and LCA to establish the mechanical performance of the materials and their life cycle impacts, respectively. The findings revealed that the condition of 10% MIBA resulted in the highest performance with slightly less compressive strength from the control. Up to 10% replacement led to insignificant strength loss but higher concentration caused strength and elastic modulus to decrease because of the failure of C-S-H and N-A-S-H gel network. Thermal stability of prepared material was observed up to 400°C and beyond 600°C due to phase decomposition. LCA showed that the impacts of Terrestrial Acidification Potential (TAP) and Marine Eutrophication Potential (MEP) were reduced by 60%, while Global Warming Potential (GWP) and water use were stable until MIBA

has been processed at high energy. The present work proves that MIBA can be employed in AAC for construction purposes as a sustainable material, mainly for structures with medium thermal resistance, and aligns with the principles of a circular economy.

CHAPTER 1: INTRODUCTION

Concrete is undeniably the most popular construction material throughout the globe and the main constituent of structures like buildings, bridges, roads, and dams. However, its production is related to severe environmental impacts. Concrete, particularly cement, which is the binder, releases almost 8% of the world's carbon dioxide (CO_2) [1]. One factor that makes cement and concrete production contribute significantly to emissions is that the cement-making process requires a lot of energy and involves heating limestone to high temperatures. Limits in the process emit sizeable amounts of CO_2. As the global population gets urbanized, infrastructure development needs to be made green through the use of cement and concrete. Alkali-Activated Concrete (AAC) has now been presented as a solution to supplement these concerns. AAC is unlike normal concrete, where the cement is replaced with industrial wastes like fly ash or slag. They alter this constructively to eradicate the related carbon emissions while making it an eco-friendly solution. Nevertheless, these advantages should be viewed together with several drawbacks, including the behavior of AAC at extreme conditions, including high temperatures, whereby applying this material in fire-prone areas should merit further study. [2–4].

In the attempt to minimize the use of OPC, there has been a lot of research on other kinds of binders. We have Fly Ash (FA), Ground Granulated Blast Furnace Slag (GGBS), Silica Fume, and Metakaolin among the studied supplementary materials. Some of these binders can be incorporated into the concrete blends in part or in whole, replacing cement and, at the same time, improving some characteristics while minimizing the impact on the environment [5,6]. Fly Ash, a waste product acquired from coal combustion, has been

18

found to enhance the workability and durability of concrete. Likewise, GGBS, a coal product in steel manufacturing, has latent hydraulic properties and is famous for increasing the close speculative effectiveness of solid-due construction. These materials, however, have some shortcomings, which are as follows. Fly Ash is another example of variable composition in which a variation in the source of coal may lead to variation in the properties of concrete. Compared to GGBS, OPC offers great strength benefits, but the latter has lower availability based on industrial activities. Furthermore, these supplementary cementitious materials have not undergone strict assessment with regard to their behavior under thermal environments, even though this is essential for understanding the applicability of these SCM in high-temperature applications, for example, in buildings that might be inflamed by fire. Therefore, there is still the need for research to strive to look for other sustainable binders that can effectively meet the building construction needs with special reference to thermal performance [7–9].

One of the most promising alternative binders that have emerged is Municipal Solid Waste Incinerator Bottom Ash (MIBA) [10]. MIBA is generated from the incineration of municipal solid waste, which comprises the refuse collected from households and industries. Typically, the residual bottom ash from incineration is disposed of in landfills, posing environmental and logistical challenges due to limited space and the potential for leaching harmful chemicals into the soil and water. However, MIBA also presents an opportunity, as its chemical composition includes silica, alumina, and various metal oxides, crucial for pozzolanic reactions. This means that MIBA when properly treated, can act as a binder that strengthens concrete through chemical reactions. Using MIBA as a partial replacement for cement or other binders helps reduce the environmental burden of waste

disposal and promotes a circular economy, where waste products are repurposed into valuable construction materials. The use of MIBA in concrete has shown promising results in improving mechanical properties, such as compressive strength and durability. Still, its performance remains underexplored, particularly in the context of elevated temperatures. Understanding how MIBA behaves under such conditions is crucial, especially for applications in buildings and infrastructure that must endure extreme heat [11–14].

A comprehensive review of existing literature reveals that the use of industrial by-products like FA and GGBS in AAC systems has been extensively documented, highlighting their benefits and limitations. Several research studies demonstrated that FA-based AAC exhibits excellent durability and mechanical properties, making it a suitable candidate for structural applications. They also found that incorporating GGBS in AAC significantly improves compressive strength due to the presence of calcium, which enhances the hydration process. In contrast, FA alone might result in slower strength development, especially at early stages, which could limit projects requiring fast construction times. Therefore, blended systems involving FA and GGBS are often recommended to balance early and long-term strength gains. While these studies have provided valuable insights into the use of FA and GGBS, only a handful of studies have explored the potential of MIBA. The preliminary tests involving MIBA as a partial replacement for cement in concrete and their results indicated that MIBA could potentially enhance thermal stability due to its high silica content, which contributes to the formation of thermally stable phases. However, the studies are limited to temperatures below 300°C, and the mechanical performance of the concrete at higher temperatures was not evaluated in detail. Studies investigated the fire resistance of concrete containing MIBA and found mixed results.

While enhanced fire resistance was indicated compared to traditional mixes, inconsistencies in the data highlighted the need for further standardization of testing protocols. Most notably, there is a significant gap in studies that address the combined mechanical and thermal performance of MIBA in AAC systems at temperatures exceeding 400°C, a scenario critical for assessing fire safety in structural applications. The lack of consistent data on MIBA's performance at elevated temperatures emphasizes the necessity for further research to validate its viability as a high-temperature-resistant material [15–17].

To address these research gaps, this study will systematically investigate the thermal and mechanical performance in alkali activated concrete with MIBA as a binder, focusing particularly on elevated temperatures. This research is novel as it investigates the use of MIBA, a relatively neglected industrial by product, as a sustainable binder in AAC systems. This study, by focusing on the combined effects of MIBA content and high-temperature exposure, attempts to shed new light on how MIBA can aid in improving both the fire resistance and the structural integrity of AAC. Experiments will be conducted using a rigorous experimental methodology by preparing high MIBA content concrete samples and performing mechanical and thermal testing under specified environmental conditions. Such findings are expected to bridge the existing knowledge gap and further demonstrate the viability of using MIBA in sustainable construction applications, providing an innovative solution to the issue of carbon emissions and the problem of eventual waste disposal.

1.1. Problem Statement

Alkali activated concrete (AAC), with a much smaller carbon footprint, compared to traditional cement-based concrete, it's an environmentally friendly alternative to traditional cement-based concrete. Which need for sustainable construction materials is increasing. However, a critical issue remains underexplored: Moreover, the behaviour of AAC at elevated temperatures is discussed in detail. Traditional concrete has well-documented properties related to fire resistance. However, AAC with MIBA as an alternative binder has not been studied in depth in fire resistance. These data are spectacularly lacking for applications in fire-prone buildings, where the construction materials' durability, mechanical properties and fire resistance are essential. It is essential to get some idea of how these materials handle high temperatures to guarantee safe and reliable deployment of AAC with MIBA in real-world applications. Since there is a research gap, this study seeks to fill it as it examines the mechanical strength, thermal properties and microstructural stability of AAC with varying amounts of MIBA to allow for critical insights into the use of AAC in sustainable and fire-resistant construction.

1.2. Aims and Objectives

The purpose of this study is to assess the performance of AAC with MIBA additions under elevated temperature conditions, with respect to its mechanical properties, fire resistance, thermal response and stability in the microstructure. The purpose of this study is to contribute to achieving insights into the suitability of AAC with MIBA as a sustainable and resilient construction material for uses in fire prone areas.

1. To investigate and assess the forensic, visual, and physical characterization of MIBA as a potential precursor substitute in alkali-activated concrete (AAC).

2. To study the forensic, visual, mechanical, mass loss characteristics, and heat Transfer of alkali-activated concrete containing municipal waste incinerator bottom ash at elevated temperatures.

3. To examine the microstructural changes and compositional transformations in alkali-activated concrete containing MIBA under elevated temperature conditions.

4. To perform a life cycle assessment (LCA) of municipal waste incinerator bottom ash as a precursor substitute in alkali-activated concrete.

CHAPTER 2: LITERATURE REVIEW

2.1   Introduction

The construction industry has been gradually shifting toward greener options, including minimizing carbon emissions and recycling by-products. Among the numerous alternatives to Portland cement-based concrete, alkali-activated concrete (AAC) has gained significant attention due to its lower carbon footprint and reliance on industrial by-products as precursors [18]. While AAC offers environmental benefits, it also exhibits mechanical properties that are equal to or superior to conventional concrete. However, in the quest for even more sustainable and durable materials, researchers have further explored additional waste-based substitutions in AAC.

One such material is municipal-waste incinerator bottom ash (MIBA), a by-product of municipal solid waste incineration that presents substantial disposal challenges [19]. The utilization of MIBA in AAC serves a dual purpose: it provides an eco-friendly waste management solution while contributing to the development of greener construction materials. Due to its high silica and alumina content, MIBA is considered a potential partial replacement for traditional AAC precursors [20]. However, its impact on AAC behavior under elevated temperatures remains underexplored.

High-temperature exposure presents a critical challenge to the durability of construction materials. Conventional concrete tends to deteriorate when exposed to extreme heat, often resulting in strength loss and structural instability [21]. In contrast, AAC has demonstrated excellent thermal resistance, primarily due to its aluminosilicate gel structure [22].

However, incorporating MIBA into the AAC matrix may modify its thermal properties, making it essential to evaluate its performance under high-temperature conditions before widespread application in fire-prone or heat-intensive environments.

Beyond waste management, integrating MIBA into AAC aligns with global sustainability objectives. By partially replacing traditional precursors with MIBA, the environmental impact of concrete production can be further reduced [23]. Furthermore, such modifications to AAC could enhance thermal resistance, leading to the development of more durable and sustainable building materials that can withstand extreme conditions. Research on MIBA in AAC bridges the gap between waste utilization and improved material performance.

Despite these advantages, concerns remain regarding MIBA's impact on the fresh and hardened properties, durability, and thermal stability of AAC. While extensive research has been conducted on the use of industrial by-products in AAC, relatively few studies have comprehensively assessed MIBA as a precursor replacement under thermal stress [23]. Addressing these knowledge gaps is crucial to advancing the development of high-performance, sustainable construction materials capable of withstanding harsh environmental conditions.

This literature review critically examines the performance of AAC incorporating MIBA, with a particular focus on its behavior under elevated temperature conditions. By synthesizing findings from high-impact research publications, this review aims to consolidate current knowledge, identify existing research gaps, and propose future directions in this dynamic field.

2.2 Alkali-Activated Concrete (AAC)

Alkali-activated concrete (AAC) is a sustainable alternative to traditional Portland cement-based concrete, utilizing industrial by-products such as fly ash (FA), ground granulated blast furnace slag (GGBFS), and metakaolin (MK) as primary binding materials. These precursors react with alkaline activators, commonly sodium hydroxide (NaOH) and sodium silicate (Na_2SiO_3), to form a geopolymer binder with high strength and durability. By reducing reliance on Portland cement, AAC significantly lowers carbon emissions while enhancing mechanical performance and durability, making it a promising material for eco-friendly construction [24]. However, its properties are influenced by factors such as precursor composition, activator concentration, and curing conditions.

The alkali activation process involves the dissolution of aluminosilicate precursors, followed by polymerization, which leads to the formation of sodium aluminosilicate hydrate (N-A-S-H) or calcium aluminosilicate hydrate (C-A-S-H) gels. These gels play a crucial role in determining AAC's strength and long-term durability. High-calcium systems, such as those incorporating GGBFS, promote the formation of C-A-S-H gels, which enhance early strength development. In contrast, fly ash-based AAC generally requires elevated curing temperatures to achieve comparable strength levels [15].

AAC demonstrates superior early compressive strength, reduced permeability, and enhanced durability compared to conventional concrete. Its dense microstructure provides excellent resistance to sulfate attack, chloride penetration, and freeze-thaw cycles [20]. Additionally, AAC performs well under high temperatures, as it lacks chemically bound water, reducing the risk of spalling. However, the incorporation of municipal-waste

incinerator bottom ash (MIBA) may alter its thermal behavior, necessitating further research to assess its stability at elevated temperatures [25].

Despite its many advantages, AAC faces certain challenges, particularly related to workability due to its high alkalinity and rapid setting time. The absence of standardized guidelines and limited long-term performance data also hinder its widespread adoption [26]. To improve economic viability and sustainability, researchers are investigating alternative waste-based precursors, such as MIBA. Furthermore, the development of ambient-cured AAC formulations could eliminate the need for energy-intensive curing methods, making large-scale applications more feasible [27].

Overall, AAC presents a viable, eco-friendly alternative to conventional concrete, balancing environmental benefits with high-performance characteristics. However, challenges related to workability, standardization, and long-term durability must be addressed for broader industry acceptance. Future research, particularly on MIBA integration and high-temperature performance, will be essential to unlock AAC's potential in sustainable construction fully [28].

2.3   Municipal-Waste Incinerator Bottom Ash (MIBA) in Construction

Municipal Waste Incinerator Bottom ash (MIBA) is a byproduct of municipal solid waste incineration and is close to 80% of total ash generated in this way. The composition of refuse derived fly ash is heterogeneous and consists of a mixture of minerals, glass, ceramics, metals, and unburned organic matter, depending on the waste type, the incineration temperature and plant-specific conditions [29]. This variability is also an obstacle to having the performance be equal on each construction application, but MIBA's

mineral-rich content makes it a potentially more promising substitute for natural aggregates and cementitious materials [30].

MIBA is being investigated as a partial replacement of fine aggregates and supplementary cementitious materials in concrete and mortar in order to reduce the environmental impact of the construction industry through the progressive adoption of industrial by-products. Studies show MIBA to enhance the compressive strength of mortar when up to 20 percent natural sand is replaced by MIBA due to improved particle packing and increased microstructure density [20]. In concrete applications, achieving comparable compressive strength to conventional concrete at 10–30% MIBA replacement levels was possible owing to calcium-rich compounds that improve pozzolanic activity and long-term strength development [31]. But MIBA performance is highly sensitive to factors such as particle size, distribution and chemical composition, and pre-treatment process [22].

Despite its advantages, MIBA presents challenges, particularly the potential leaching of heavy metals, which raises environmental concerns [28]. Pre-treatment techniques such as washing, sieving, and carbonation play a crucial role in reducing contamination and improving its overall stability [19]. Additionally, MIBA's high water absorption can negatively impact concrete workability, requiring mix design adjustments to maintain consistency and strength [24]. The variability in its composition further leads to inconsistencies in performance, underscoring the need for standardized testing and stringent quality control measures [25].

The integration of MIBA into construction materials supports sustainability by diverting waste from landfills and reducing the depletion of natural resources. Its partial substitution

for aggregates and cement contributes to lowering CO_2 emissions from cement production, aligning with global efforts to promote greener construction practices [15]. Economically, MIBA presents cost-saving opportunities by reducing disposal expenses while fostering a circular economy [26]. However, comprehensive studies on its long-term durability, including resistance to freeze-thaw cycles, fire performance, and structural reliability, are necessary to establish its feasibility for widespread use in construction [27].

MIBA is a viable, sustainable alternative to the construction sector which provides both eco-nomic and environmental benefits. However, greater work is needed in overcoming material variability, heavy metal leaching, and long-term durability. MIBA has great potential as a key material in sustainable building construction, especially when properly pre-treated and following appropriate regulations, which would set this application apart by reducing waste and improve build material performance [23].

2.4   Effects of Elevated Temperatures on Alkali-Activated Concrete (AAC)

Alkali-Activated Concrete (AAC) is gaining recognition for its exceptional fire resistance compared to conventional Portland cement-based concrete. Its unique aluminosilicate gel structure provides high thermal stability, making it particularly suitable for fire-prone environments and high-temperature applications [17]. Understanding AAC's behavior under extreme heat is crucial for ensuring its long-term durability and structural integrity.

Research indicates that AAC retains a significant portion of its strength even at temperatures reaching 800°C, primarily due to its stable geopolymer gel. Unlike traditional concrete, which suffers strength degradation and spalling due to the decomposition of calcium hydroxide, AAC maintains its structural integrity under thermal exposure.

29

Moreover, incorporating steel fibers can further enhance AAC's fire resistance by mitigating strength loss and improving thermal stability [32].

The microstructure of AAC densifies at moderate temperatures and improves the mechanical performance as a result. That said, the material can become weakened by thermal stress and dehydration, and microcracks will occur at temperatures more than 400°C. Due to its role in subduing crack formation, adding steel fibers provides a means of enhancing AAC's ductility as well as overall stability under severe heat conditions [17].

AAC has higher thermal resistance than ordinary Portland cement (OPC) concrete. Rapid strength loss of OPC concrete occurs because of the decomposition of hydration product under high temperatures; in contrast, AAC without such compounds retains its structural integrity. AAC becomes a more reliable construction material for fire-resistant as well as high-temperature applications [33].

AAC's performance under elevated temperatures highly depends on the curing method as well. The high thermal resistance shown by ambient cured AAC is, however, differentially sensitive to the composition and mix design of the precursor materials. Additionally, curing techniques can further optimize its resilience, making AAC even more viable option for high-temperature structural applications [28].

In essence, AAC is an excellent, fire-resistant alternative to standard concrete. Additives, fiber reinforcement and optimized curing methods may further improve its performance. As research continues to advance, AAC's potential application in fire-resistant structures and extreme heat environments is becoming wider and wider [26].

2.5 Influence of MIBA on AAC at Elevated Temperatures

The incorporation of MIBA into AAC presents a sustainable and innovative approach to improving thermal performance while reducing environmental waste. MIBA has the potential to increase the fire resistance of AAC when compared to traditional concrete, and AAC already has better fire resistance than traditional concrete [34]. It is, however, lacking long-term thermal behaviour and chemical interaction understanding for optimizing mix design and structural reliability.

2.5.1. Thermal Stability and Mechanical Performance

Research indicates that AAC incorporating MIBA retains a significant proportion of its compressive strength even at temperatures up to 800°C, mainly due to the formation of stable geopolymeric gels that resist thermal degradation. The pozzolanic nature of MIBA enhances the formation of calcium-aluminosilicate hydrates (C-A-S-H), which improve fire resistance and long-term strength [32,35]. However, when exposed to temperatures exceeding 400°C, thermal stresses and moisture loss can induce microcracks, compromising structural integrity. The addition of steel fibers has been shown to mitigate these effects, enhancing ductility and thermal stability [25].

The interaction of MIBA with alkaline activators is another critical factor influencing its performance at elevated temperatures. Studies have shown that higher molarity NaOH solutions (8M–12M) improve strength and reduce porosity by forming denser N-A-S-H gels, which are crucial for thermal resistance [36]. However, excessive alkali concentrations can trigger aluminum corrosion, leading to aeration and increased porosity, which negatively impacts mechanical performance [37].

2.5.2. Microstructural Evolution and Mix Optimization

The microstructural behavior of MIBA-modified AAC under high temperatures requires further investigation. Advanced characterization techniques such as SEM and XRD can provide valuable insights into reaction product formation and their impact on thermal stability [38]. Recent studies indicate that CO_2 curing at elevated temperatures enhances compressive strength and helps mitigate porosity issues caused by hydrogen gas evolution from reactive aluminum in MIBA-based AAC [39].

Moreover, the partial replacement of fly ash (FA) with MIBA has been shown to increase porosity and reduce compressive strength, necessitating optimized mix proportions to maintain structural integrity [40]. Some studies have also evaluated the carbonation resistance of MIBA-based AAC, with findings suggesting that while it may perform poorly under accelerated carbonation, it demonstrates enhanced durability under natural environmental conditions due to its anti-diffusion properties [41]. Additionally, waste glass powder has been explored as a complementary precursor to MIBA, as its high reactive silica content enhances geopolymerization, resulting in low thermal conductivity and improved mechanical properties making it a viable option for energy-efficient and fire-resistant construction [42].

2.5.3. Environmental Considerations and Practical Challenges

Despite its potential, the use of MIBA in AAC presents several challenges, particularly related to material consistency, heavy metal leaching, and long-term durability. Pre-treatment methods such as alkaline washing have been suggested to remove metallic aluminum, reducing hydrogen gas formation and improving pozzolanic activity [43].

Modifying mix proportions or incorporating accelerated CO_2 curing may enhance mechanical and thermal properties while minimizing environmental risks [44]. Studies have examined the high-temperature resistance of AAC slag composites with varying MIBA substitution levels (0%–12%), identifying that a 6% MIBA replacement offers optimal thermal and mechanical performance. However, increasing MIBA content beyond this threshold can lead to excessive porosity and reduced strength due to gas evolution and inconsistent reactivity [45].

2.6   Gaps in Existing Research and Future Perspectives

The use of MIBA in AAC has gained attention for its environmental and economic benefits. However, several research gaps must be addressed before it can be widely adopted, particularly concerning its performance under elevated temperatures [30]. Current studies mainly focus on mechanical properties at ambient conditions, but long-term durability under high temperatures remains underexplored. The effects of thermal cycling, spalling, and degradation over time must be thoroughly investigated to ensure structural stability in fire-prone environments [20]. Similarly, microstructural transformations in MIBA-AAC at high temperatures require deeper analysis. Advanced techniques like scanning electron microscopy (SEM) and X-ray diffraction (XRD) can help correlate microstructural changes with material performance [31]. Another challenge is the lack of standardized mix designs and curing protocols. Variations in MIBA composition, alkaline activator concentration, and curing conditions lead to inconsistent performance, making it difficult to implement MIBA-AAC in real-world applications [46]. Additionally, concerns about heavy metal leaching, especially at high temperatures, need comprehensive environmental impact assessments to ensure the material's safety and regulatory compliance [19].

Future research should take a multidisciplinary approach to bridge these gaps, integrating materials science, structural engineering, and environmental studies. LCA will also provide a clearer picture of sustainability benefits [25]. Collaborative efforts are needed to develop optimized MIBA-AAC formulations that ensure thermal performance, durability, and environmental safety [25]. Addressing these research gaps is essential for MIBA-incorporated AAC to become a mainstream sustainable construction material. Focused investigations into long-term durability, standardization, and environmental safety will pave the way for its large-scale adoption, contributing to fire-resistant and eco-friendly infrastructure [18].

2.7   Summary

AAC represents a sustainable alternative to Portland cement-based concrete and has environmental and mechanical advantages. The addition of MIBA increases sustainability and benefits mechanical properties, pozzolanic activity, thermal resistance carbon emissions and landfill waste. Its geopolymer gel matrix provides AAC superior fire resistance up to 800°C as demonstrated by the integrity of the material. However, at extreme temperatures of greater than 400°C, microcracks and pore coarsening develop, and material shrinkage occurs. The long-term durability and performance under thermal cycling are still incomplete, but steel fiber reinforcement mitigates cracking. However, heavy metal leaching under heat remains a concern with MIBA reducing reliance on raw materials reducing costs and environmental impacts. For large scale adoption, mix design, curing protocols, and conducting LCAs, field tests and toxicity assessments are critical.

CHAPTER 3: MATERIALS AND METHODS

3.1. Materials

3.1.1. Fly ash (FA)

The FA used in this study was a low-calcium class F sourced from a local thermal power station. The use of this particulate type of fly ash has been informed by its high alkali content, making the material suitable for polymerization in the production of rubberized geopolymer concrete. Consequently, the chemical composition of the oxide in the FA was analysed through XRF summarising the alloy composition variation in Table 4.1. and the crystalline phase was identified through XRD. This fly ash played a pivotal part in the total mixture design and is used to achieve the required characteristics of geopolymer concrete blends formulated in this study.

3.1.2. Ground granulated blast furnace slag (GGBFS)

The GGBFS that was used in this work was purchased from the local market, thus has been made sure that the properties used are standard. GGBFS is fine, reactive powder produced from industrial waste born during iron production in which molten slag congeals with water/steam to tiny bulks. In this research, GGBFS was one of the predominant activators and raw materials needed to prepare AAC. Its chemical composition was determined using XRF as shown in Table 4.1, and the crystalline phase was identified through XRD, which cumulatively shows that it is suitable for geo-polymerization. Being a constituent of the binder system, GGBFS transforms, with the aid of alkaline activators, into a stable and strong matrix for the concrete, improving its mechanical and durability characteristics.

These properties of GGBFS affected the conventional properties of the rubberized geopolymer concrete mixes, leading to the structural and sustainable aspects they possess.

3.1.3. Municipal-waste Incinerated Bottom Ash (MIBA)

Municipal Waste Incinerated Bottom Ash (MIBA) procured from the local market in processed form was used as secondary material in the AAC mixture. MIBA is produced during the burning of municipal solid waste and has reactive oxides that play a role in the geo-polymerization of raw materials. Before being used, the MIBA was processed, and then, the XRF, XRD, TGA and FTIR characterisation was performed with a specific gravity of 2.78. The integration of MIBA was proposed to enhance the mechanical properties and sustainable qualities of concrete and at the same time, reduce waste in construction material.

3.1.4. Fine & Coarse aggregate

The fine and coarse aggregates were crucial in determining the AAC's workability, cohesiveness, and overall performance. River sand was chosen as the fine aggregate because its properties were uniformly tested for the most appropriate concrete performance. The fineness modulus, specific gravity, and water absorption were determined based on ASTM guidelines to be 2.66, 2.6, and 1.3%, respectively.

Likewise, the coarse aggregate used in this study was obtained from a Margalla quarry and played a major role in the mechanical and structural characteristics of the final concrete product. The coarse aggregate's specific gravity and water absorption were found to be 2.74 and 1.28%, respectively, in compliance with set quality standards. These results confirmed

that the selected river sand and coarse aggregate satisfied the regulatory agency standards and were acceptable for use in the geopolymer concrete mix.

3.1.5. *Sodium Hydroxide & Sodium Silicate*

The alkali activators, Sodium hydroxide (NaOH) and Sodium silicate (Na_2SiO_3) needed for the alkali activation of FA and GGBFS in this study were obtained from the local market. Several studies pointed out that sodium hydroxide increases the solubility of aluminosilicate precursors. In contrast, sodium silicate is responsible for polymerization and shares a role in forming mechanical strength. In this work, NaOH solution with a 12M molarity was prepared, and Na_2SiO_3 was added at a 2:1 ratio to enhance the reactivity of the binder. The correct proportion of those activators was used in this research to obtain desirable workability, setting time, and compressive strength of the AAC.

Figure 3.1: Sodium Hydroxide & Sodium Silicate used for this study

3.1.6. *Superplasticizer*

The high-range water-reducing superplasticizer was chosen to improve the workability and flowability of the AAC. It enhances slump flow and early and ultimate compressive

strengths by affecting powder dispersion and reducing water demand. In this study, 5% of the total cementitious material has been considered the dosage of SP.

3.2. Methodology

3.2.1. Mix Design

The mix design for AAC was based on established methodologies from previous studies [47,48]. The AAC mix consisted of an equal blend of FA and GGBFS. All concrete samples maintained a consistent ratio of precursors to aggregates at 1:3, precursors to sand at 1:1.5, and an alkali activator (AA) to precursor ratio of 0.5 by mass.

The alkali activator solution was prepared using water, NaOH (99% purity), and Na_2SiO_3. The NaOH solution (12M) had a composition of 52% water and 48% NaOH, while Na_2SiO_3 was added at twice the mass of NaOH. Potable tap water was used for mixing all specimens. Additionally, a high-range water-reducing superplasticizer (SP) was incorporated at 5% of the total precursor weight across all mixes to enhance workability. Table 1 outlines the material composition for 1m³ of concrete. The control mix, labelled M00, contained no MIBA. Modified mixes, labelled M05, M10, M15, and M20, incorporated 5%, 10%, 15%, and 20% MIBA by weight, respectively, replacing an equivalent portion of FA (95%, 90%, 85%, and 80%, respectively). This systematic mix design ensured consistency while allowing for the evaluation of MIBA's effects on AAC performance.

Table 3.1: Mix Design of AAC used in the study

Sample/Ingredients	FA	MIBA	GGBFS	Sand	CA	NaOH	Na₂SiO₃	SP
M00 (Control)	1150	0	1450	2400	4500	218.3	466.6	130
M05	1092.5	57.5	1450	2400	4500	218.3	466.6	130
M10	1035	115	1450	2400	4500	218.3	466.6	130
M15	977.5	172.5	1450	2400	4500	218.3	466.6	130
M20	920	230	1450	2400	4500	218.3	466.6	130

3.2.2. Alkaline Activator

Preparation of a 12-molar solution of NaOH and incorporation of Na_2SiO_3 at a concentration twice that of NaOH was the methodology. First, the dry FA and GGBFS were mixed to a fine powder and then gradually NaOH solution was mixed to activate the alkaline reaction. The Na_2SiO_3 solution was then added to the mixture at a ratio of twice that of NaOH, as that is enough to ensure sufficient silica content.

Figure 3.2: Preparation of Alkaline activator solution

3.2.3. Collection and Pre-treatment of MIBA

MIBA is derived from a municipal solid waste combustion facility, a byproduct of municipal solid waste combustion. It is then collected, inspected and prepared so that it is fit for use in AAC. Visible impurities are removed by manual inspection, like large metallic fragments, plastics and organic material. Further cleanup of material is obtained by utilizing magnetic separation to remove ferrous materials. The aim of this step was to remove magnetic particles which might interfere with AAC reactivity and structural integrity. After this, Los Angeles abrasion equipment for ball milling is used to reduce MIBA to particle size. For fine particle generation to promote reactivity in alkali activation, this process is carried out for two hours. The MIBA is milled and sieved through a 200 sieve from which only the fraction that passes through is further characterized and used for experimental work.

Manual Cleaning   Milling through Los Angeles Abrasion Machine   Sieving #200   Sieve #200 Pass

Figure 3.3: Preparation methodology of MIBA for study

3.2.4. Characterization of Materials

The chemical composition, mineralogical structure and thermal behaviour of MIBA are fully characterized to understand MIBA. Key characterization techniques include:

- X-Ray Fluorescence (XRF): Used to determine the elemental composition of MIBA, including silicon, aluminium, calcium, and other oxides essential for alkali activation.
- X-ray diffraction (XRD): Applied to identify the crystalline phases and mineral components within MIBA, such as quartz or unburnt residues.
- Scanning Electron Microscopy (SEM): Provides microstructural images to study particle morphology and surface features.
- Thermogravimetric Analysis (TGA): Evaluates the thermal stability and decomposition behaviour of MIBA under increasing temperature conditions.
- Fourier Transform Infrared Spectroscopy (FTIR): This technique identifies functional groups present in MIBA that may influence its reactivity.

Figure 3.4: MIBA sample preparation for XRF analysis

3.2.5. Preparation of Alkali-Activated Concrete

The AAC is prepared with a blend of MIBA with FA and GGBFS as the primary precursors. MIBA is incorporated as a partial replacement for FA at varying levels of 5%,

10%, 15%, and 20% by weight. The alkaline activator solution is prepared using 12M sodium hydroxide (NaOH) and sodium silicate (Na_2SiO_3) in a 1:2 ratio by weight.

The mixing process begins with the precursors and MIBA being dry-mixed to ensure uniform distribution. The alkaline solution, prepared 24 hours in advance, is gradually added to the dry mix while maintaining consistent mixing speed. This ensures homogeneity in the fresh AAC mixture, which is then cast into molds of specific dimensions for testing.

Figure 3.5: (a) Mixing and casting of AAC sample (b) sample with a thermocouple for temperature measure during elevated temperatures

3.2.6. Curing Regime

The specimens were demolded after 24 hours and subjected to heated curing of the sample, which took place for 72 hours in the heated environment at 60±5℃ and then at ambient temperature for 28 days (Auxilia Rani & Sudha, 2024)Ambient curing is chosen to mimic real-world conditions, making the results more applicable to practical use. After the casting and curing period, the samples were exposed to certain tests.

Figure 3.6: Casted sample and their heated curing in oven

3.2.7. Exposure to Elevated Temperatures

To evaluate the thermal performance of AAC with MIBA, the cured specimens (after 28 days) were exposed to elevated temperatures of 24°C (ambient), 200°C, 400°C, 600°C, and 800°C. Each temperature exposure is maintained for one hour using a controlled furnace with the heating mechanism detailed in below Figure 3.7. This phase simulates fire scenarios and tests the material's ability to withstand thermal stresses.
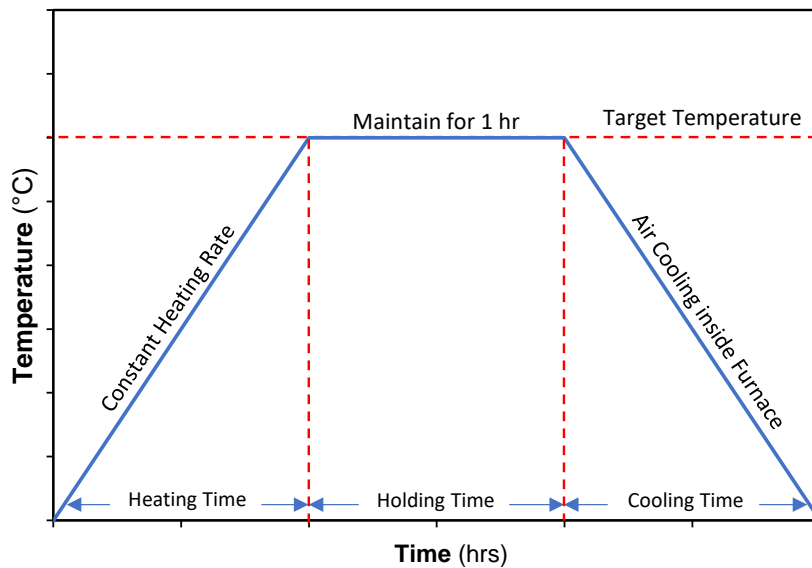
Figure 3.7: Heating process of AAC samples in furnace
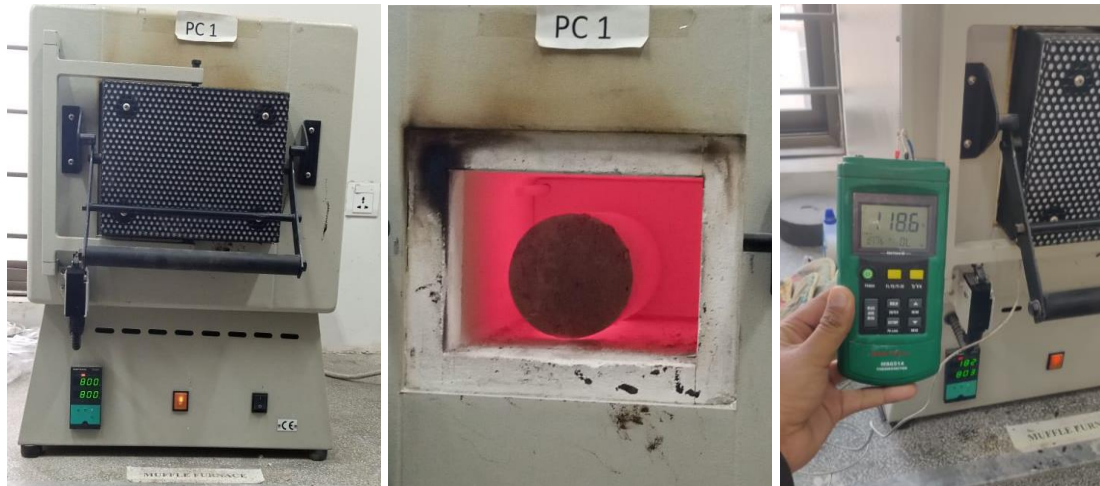
Figure 3.8: Furnace heating and measurement of core temperature using thermocouple

3.2.8.   Performance Evaluation of AAC

The AAC specimens are exposed to high temperatures, followed by mechanical and thermal performance tests. These include:

- Mass Loss Measurement: It considers its weight reduction due to dehydration and decomposition of material.

- Dry Density Testing: It determines the changes in density after thermal exposure and shows changes indicating structural stability.

- Ultrasonic Pulse Velocity (UPV): A test used for evaluation of internal defects or cracks without destruction.

- Heat Transfer Testing: Insulation properties of AAC under various thermal conditions are measured.

- Compressive Strength Testing: Provides an evaluation of AAC's mechanical performance and load bearing capacity.

- Microstructural Analysis: SEM and XRD analyses are used for phase changes, microcracking and other microstructural alteration occurring at elevated temperature in specimens.

Figure 3.9: Sample testing through compression machine and SEM

3.2.9. Life Cycle Assessment (LCA)

The impact of MIBA in AAC is quantified by means of a life cycle assessment in order to determine its environmental benefits. Sensitivity analysis of MIBA processing, AAC production and thermal performance, and their energy consumption and carbon footprint were evaluated. Further, the LCA shows the reduction in the use of natural resources that results from the partial replacement of the FA by the MIBA and makes clear a holistic view of the material's sustainability.

3.2.10. Testing Matrix

A range of temperature conditions were used to assess the performance of AAC with MIBA incorporation in the experimental program. Five AAC mix designs (M00, M05, M10, M15 and M20) were used in the testing matrix, interchangeably substituting Fly Ash with MIBA at 0, 5, 10, 15 and 20% by weight (see Table 3.2). Ambient temperature (24°C) and elevated

temperature (200°C, 400°C, 600°C, and 800°C) were used as evaluation temperatures for these mixes. For each temperature condition a set of three cylindrical specimens (4'in' diameter and 8'in' high) were prepared yielding nine 90 samples to be tested. Mass loss analysis, ultrasonic pulse velocity (UPV) measurements and compressive tests were key assessments on the thermal stability and mechanical performance of AAC. Importantly, thermocouples were also incorporated into the samples for use in heat transfer tests to quantify the insulating characteristics of the material. The high quality of this matrix allowed a detailed investigation of the effect of MIBA replacement on both the thermal and mechanical properties of AAC.

Table 3.2: Testing matrix for the study

Sample\ Temp.	Mass Loss: UPV & Compression					Heat Transfer
	24°C	200°C	400°C	600°C	800°C	
M00	3	3	3	3	3	3
M05	3	3	3	3	3	3
M10	3	3	3	3	3	3
M15	3	3	3	3	3	3
M20	3	3	3	3	3	3
All samples were 4 in Diameter and 8 in height					Total	90

3.2.11. Summary

The results from this experimental program (flowchart presented in Figure 3.10) are put forth as helpful to our understanding of MIBA's contribution to AAC production and its behavior under elevated temperatures. In addition, the study tries to fill the gap in the current literature on the use of MIBA in AAC and proposes a path for its utilization as a sustainable construction material.
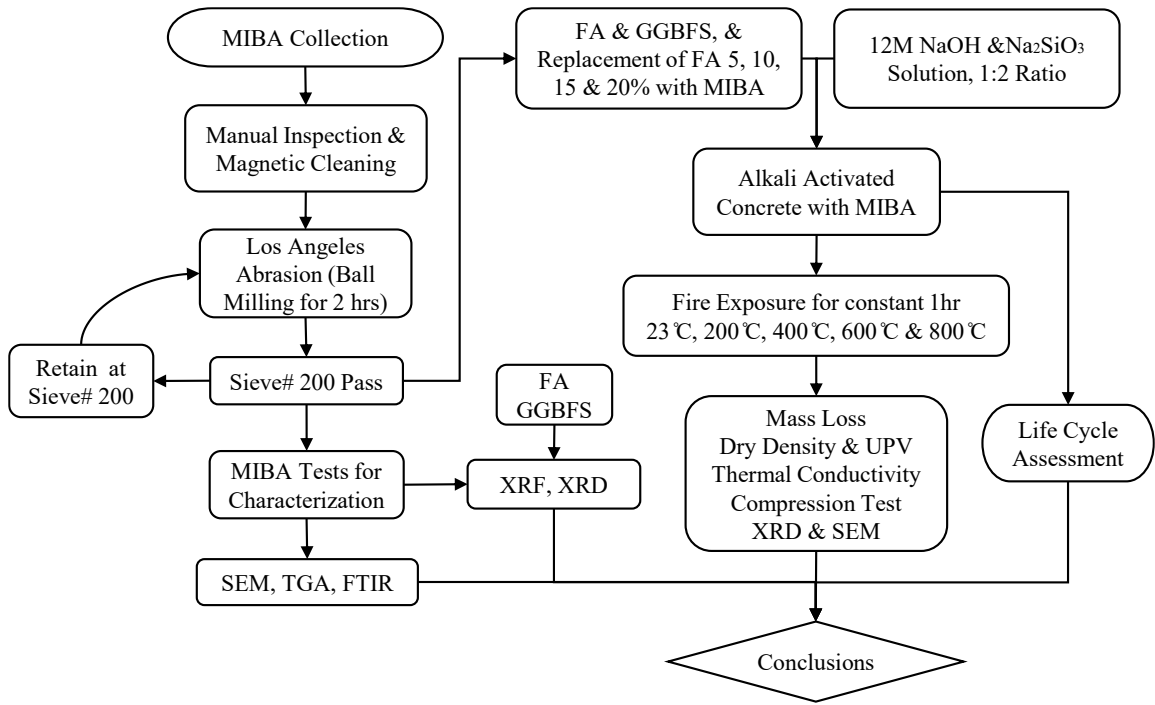
Figure 3.10: Methodology of the study

CHAPTER 4: RESULTS AND DISCUSSION

4.1. MIBA Characterization

4.1.1. XRD and XRF Analysis

The XRD pattern of FA indicates quartz, calcite, hematite, and corundum as major peaks indicating. The dominant phase here is Quartz, exhibited in peaks around 26.5° and 20.9°, calcite is seen in peaks around 29.5°. Less intensity of hematite and corundum is also present. Fly ash is well known as an active pozzolanic material in the understanding of AAC. Fly ash is involved in formation of calcium silicate hydrate (C-S-H) when it is alkali activated. This critical phase improves significantly the mechanical properties and long-term durability of the concrete. In most peaks, MIBA has a higher crystalline phase than FA, including quartz and calcite at the calculated angle of 26.5° and 29.5°, respectively. Hematite and corundum are detected but make a less pronounced contribution. The elevated crystalline content of MIBA implies a lower inherent reactivity, requiring supplemental processing to make MIBA more suitable for AAC use. However, despite this, existing research supports MIBA as appropriate for use in AAC to form binding phases during alkalis activation. The unique crystalline profile of GGBFS is revealed by the XRD analysis, which shows peaks corresponding to quartz, calcite, and minor hematite phases. Finally, GGBFS latent hydraulic properties are underscored by the relatively lower intensity of quartz peaks compared to FA and MIBA, and the presence of calcite. At a more practical scale (clay components), these properties are activated in the presence of alkalis, resulting in the formation of C-S-H and other hydration products, which considerably improve the strength and durability of AAC.

48

The XRF analysis of MIBA, FA, and GGBFS precursor materials is shown in Table 4.1. Since the MIBA and GGBFS are both rich in calcium oxide (CaO), which will result in the formation of strong binding phases, such as calcium silicate hydrate (C-S-H), therefore these two materials will be very useful in helping to form water for structurally strong concrete. However, FA, with lower CaO, is expected to improve long term durability of the concrete via its pozzolanic reaction. Also, it has a very high amount of silicon dioxide (SiO_2), which is all important in the formation of the silicate structures that bind the concrete together. Also, the high amount of aluminium oxide (Al_2O_3) in fly ash will serve to create aluminosilicate networks, making the concrete more resistant to chemical attack. At the same time however, the moderate SiO_2 and Al_2O_3 levels in MIBA and slag will help keep the overall structure less pronounced thereby giving the concrete a strength and flexibility. Microstructure of concrete will also be influenced by other oxides like Fe_2O_3, MgO and SO_3 and will contribute to its durability, weather resistance etc. When the mix proportions is considered the use of a robust alkaline solution and the high temperature curing process, the AAC generated is shown to be both strong and durable and hence suitable for use in challenging structural applications.
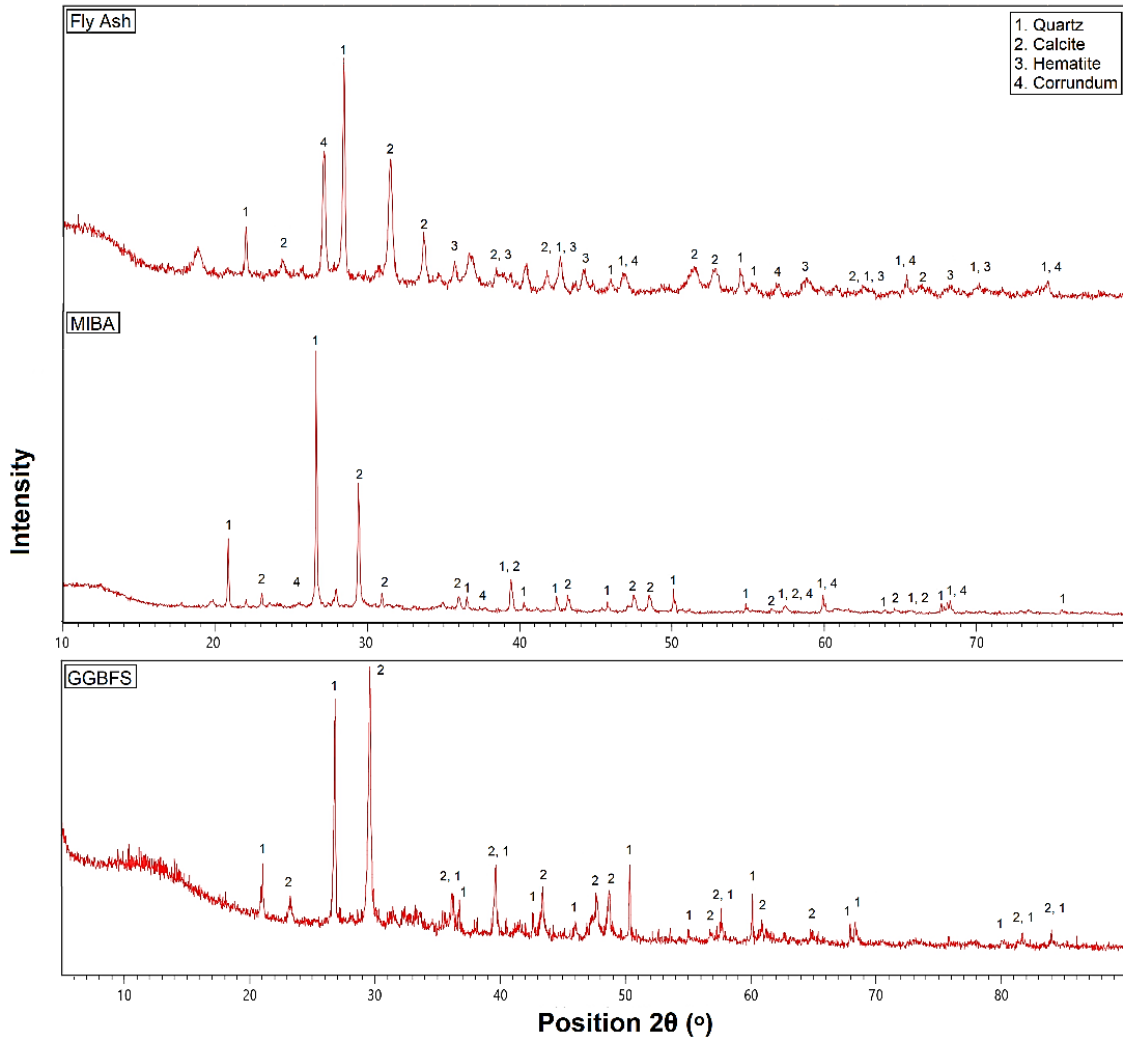
Figure 4.1: X-ray Diffraction (XRD) spectrum of FA, MIBA and GGBFS

Table 4.1: XRF Analysis of different precursors used in AAC

| Mineral (%)	CaO	SiO$_2$	Al$_2$O$_3$	Fe$_2$O$_3$	SO$_3$	MgO	K$_2$O	Na$_2$O	P$_2$O$_5$	Others	LOI
MIBA	44.54	21.86	7.48	4.47	2.55	2.79	1.63	1.98	0.00	0.01	12.6
FA	4.53	49.16	31.51	6.23	1.31	0.52	1.41	0.50	0.48	0.41	4.12
GGBFS	31.94	29.18	6.62	7.65	3.53	3.98	0.00	1.05	0.075	0.80	15.9

4.1.2. Fourier Transform Infrared Spectroscopy (FTIR)

Figure 4.2 shows the Fourier Transform Infrared Spectroscopy (FTIR) spectrum of MIBA that shows several key functional groups and chemical bonds associated with its composition. The presence of moisture or hydroxylated minerals such as portlandite $(Ca(OH)_2)$ is evidenced by the broad absorption band in the region of $3400cm^{-1}$ which is ascribed to the stretching vibrations of hydroxyl groups (O-H). Moreover, the peculiar absorption bands ($1450–1500$ cm^{-1}) revealed are related with bending vibrations of carbonate groups (C-O) that can be attributed to the presence of carbonate compounds (carbonate $CaCO_3$). The spectrum is characterized by a number of prominent bands in the range 1000-1100 cm^{-1} which are associated with the asymmetric stretching vibration of Si-O-Si or Al-O-Si bonds and so reflect silicate or aluminosilicate phases common in ash materials attributable to their glassy silicate content. Small peaks at 870 cm^{-1} and 700 cm^{-1} show the existence of the crystalline silicates quartz. The FTIR analysis indicates that MIBA is composed of combinations of hydroxylated, carbonated and silicated compounds, which constitutes its complex mineralogical composition.

4.1.3. Thermogravimetric Analysis (TGA)

The TGA of MIBA in Figure 4.3 gives valuable information about thermal stability and decomposition behaviour in the presence of increased temperature. The evaporation of free as well as physically bound water is elucidated by the TGA curve, which shows an initial slow weight loss up to approximately 200°C. A more pronounced weight loss continues between 200°C and 400°C, due to decomposition of the hydrated phases such as portlandite $(Ca(OH)_2)$ and other similar minerals. The greatest weight loss is estimated to occur

between 600 °C and 800 °C since carbonate compounds decompose at this temperature, resulting in the release of carbon dioxide (CO_2) from decomposing calcite ($CaCO_3$). At temperatures higher than 800°C, the curve shows a slower decrease in weight, possibly due to the decomposition of more stable mineral phases or the transformation of silicate phases; the behavior of MIBA, also found in the literature [49–52], is also discussed. The thermogravimetric profile indicates that MIBA contains many volatile compounds encompassing water, carbonates, and hydrated minerals, which decompose at elevated temperatures. These thermal properties, on which the heat-treated MIBA products depend for their structural properties and durability, must be understood to give insight into their ability to affect the porosity, strength and durability of MIBA types in construction materials.[49–52].
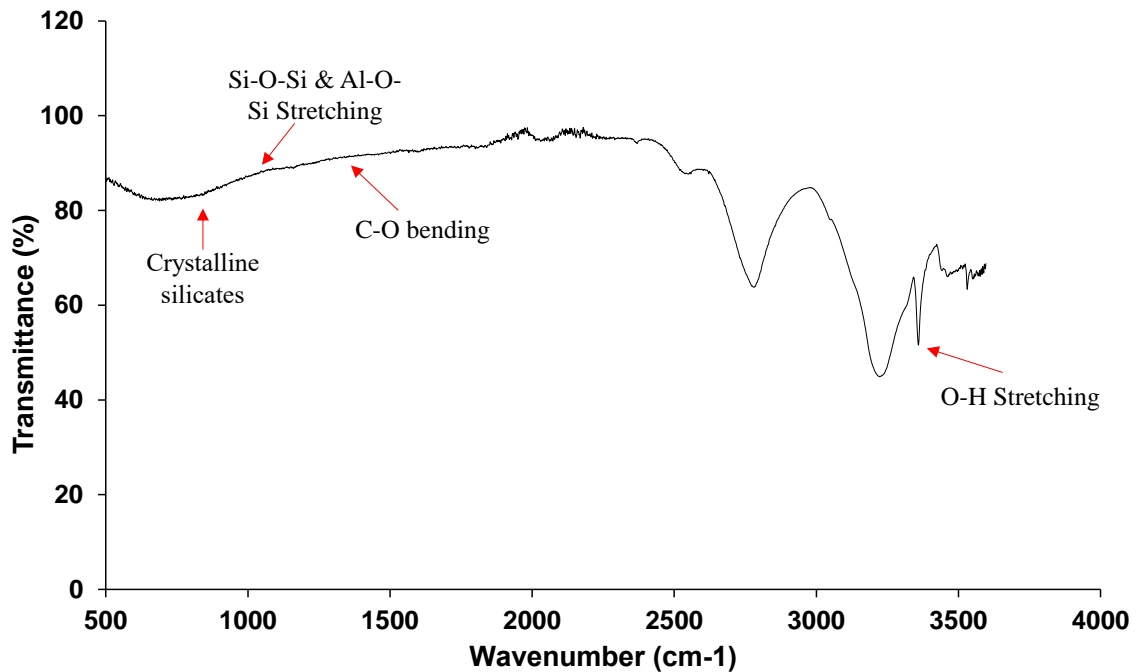
Figure 4.2: FTIR spectrum of MIBA
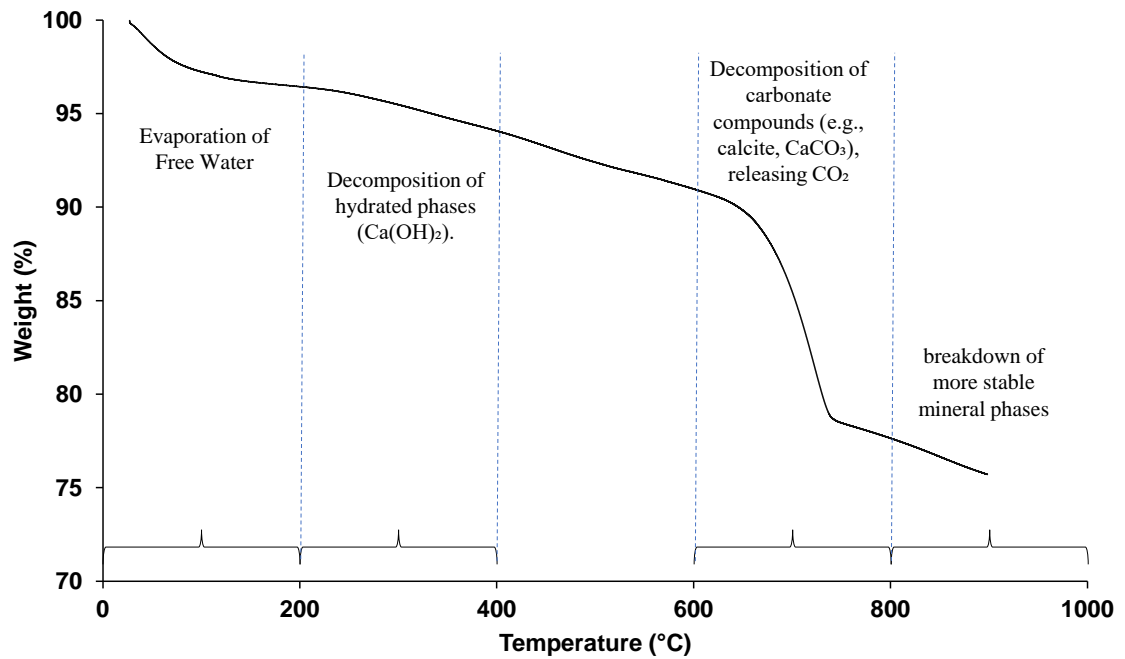
Figure 4.3: TGA spectrum of MIBA

4.1.4. SEM Analysis of MIBA

Figure 4.4 shows the SEM image of ash that particles seen in Figure 4.4 are irregular in shape and varying in size, which is characteristic for bottom ash because of the heterogeneous origin of the particles as well as of the ash processing during incineration. Composition differences are indicated by varying brightness of the particles. Their brightness suggests that brighter areas tend to reflect more electrons and could mean that the material is more atomic number, or denser. The EDS analysis corroborates with this and we know the particles are bright and heavy, so they must comprise metallic elements. The elements were detected by energy-dispersive spectroscopy (EDS): carbon (C), oxygen (O), silicon (Si), aluminium (Al), sodium (Na), magnesium (Mg), potassium (K), calcium (Ca), and iron (Fe). There were some notable constituents which included the weight

percentage of the main components which were found to be carbon and oxygen, the highest weight percentage; as both constituents are commonly found in several organic, and inorganic materials. Silicon, aluminium and calcium hint at the existence of silicate minerals or aluminosilicates like ash residues. The result of this test indicated that municipal waste bottom ash is comprised of a variety of elements, carbon, oxygen, silicon and calcium present in abundance among others. This ash composition is representative of waste ash generated from the combustion of a mixed waste source consisting of biodegradable materials in addition to noncombustible inorganic materials. Municipal waste is distinct, however, in that it can contain so-called 'elements', metals like aluminium, sodium, magnesium, potassium, and iron, along with packaging materials, construction debris, and household items.
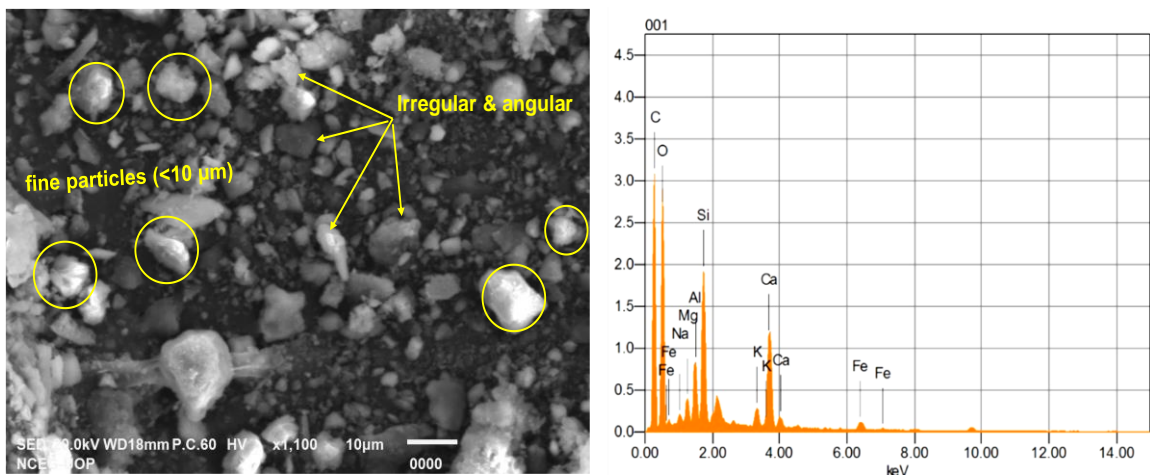
Figure 4.4: SEM and EDX Analysis of MIBA

4.2. Analysis of Color Variations in AAC with MIBA Incorporation

Chemical and physical transformations during thermal exposure produce color variations in AAC with FA, GGBFS and different percentages of MIBA. Such transformations are a

function of the material composition, including calcium oxide (CaO), iron oxides (Fe_2O_3), silicon dioxide (SiO_2), and alumina (Al_2O_3) and phase transformations, oxidation, and dehydration. Figure 4.5 details the chemical process of AAC samples (M0 to M20) and the color behavior change from room temperature to 800°C and comparses the color changes in the same sample in different temperatures.

4.2.1. Room Temperature (23°C): Initial Dark Gray Appearance

The AAC samples (M0, M05, M10, M15, and M20) exhibit a uniform dark gray color at ambient conditions. This coloration is primarily due to the presence of unreacted materials such as FA, GGBFS, and MIBA. The iron oxides (Fe_2O_3) in MIBA impart a darker tone, while the silicate and alumina content in FA and GGBFS initiate the formation of early gel phases, such as C-S-H (calcium silicate hydrate) and N-A-S-H (sodium aluminosilicate hydrate).

Among the samples, M0 (0% MIBA) shows a slightly darker hue compared to M20 (20% MIBA), as MIBA introduces calcium-rich compounds that slightly dilute the impact of iron oxides. The uniformity across samples indicates that, at this stage, no significant chemical changes or thermal degradation processes have occurred.

4.2.2. 200°C Exposure: Slight Lightening Due to Dehydration

Upon exposure to 200°C, all samples begin to lighten slightly, particularly those with higher MIBA content (M10, M15, M20). This is attributed to the dehydration of bound water in the gel phases (C-S-H and N-A-S-H), which reduces the material's water content and density.

- **M00:** Shows minor lightening, retaining much of its original dark gray tone.

- **M20:** Exhibits more pronounced lightening, reflecting the greater influence of MIBA's high CaO content. Calcium-rich phases begin to dominate, contributing to lighter colors.

Additionally, minor oxidation of Fe^{2+} compounds to Fe^{3+} begins, though its impact on color is limited at this temperature. This phase marks the onset of physical changes, with the material becoming less dense and slightly more brittle.

4.2.3. 400°C Exposure: Pronounced Discoloration and Phase Formation

At 400°C, significant discoloration is observed, with samples transitioning to whitish and brownish tones. The changes are most prominent in M10, M15, and M20, which have higher MIBA content.

- **M00:** Begins to show whitish patches as dehydration intensifies and crystalline phases like gehlenite ($Ca_2Al_2SiO_7$) start forming.

- **M20:** Exhibits a mixture of whitish and brownish discoloration due to the higher CaO and Fe_2O_3 content, leading to the oxidation of iron compounds and the decomposition of sulfates (SO_3).

The chemical transformations at this stage include the decomposition of early gel phases and the formation of crystalline phases, such as gehlenite, which are more stable at elevated temperatures. The oxidation of Fe^{2+} to Fe^{3+} intensifies, contributing to the brownish hues in samples with higher MIBA content.

4.2.4. 600°C Exposure: Beige to Reddish-Brown Tones

At 600°C, the AAC samples develop distinct beige to reddish-brown tones. The progression of color in the same samples highlights the increasing influence of oxidation and high-temperature phase formation.

- **M00:** Turns a light beige color, primarily due to the complete dehydration of gel phases and the dominance of silicate-rich crystalline phases.

- **M20:** Shows a reddish-brown tone, reflecting the significant oxidation of Fe^{2+} to Fe^{3+} and the formation of high-temperature phases like anorthite ($CaAl_2Si_2O_8$).

The decomposition of volatile compounds, indicated by MIBA's high LOI (Loss on Ignition), contributes to porosity and microstructural changes. Sulfate decomposition further alters the material's texture, with visible cracks beginning to form in samples with higher MIBA content.

4.2.5. 800°C Exposure: Uniform Light Beige with Surface Cracks

At 800°C, all samples display a uniform light beige to pale brown color, with visible cracking, particularly in M15 and M20. The progression of color from 23°C to 800°C shows the culmination of dehydration, oxidation, and crystallization processes.

- **M00:** Retains its light beige tone, with stable crystalline phases like mullite ($3Al_2O_3 \cdot 2SiO_2$) dominating its structure.

- **M20:** Becomes paler but more porous, with increased surface cracking due to the high CaO and Fe_2O_3 content in MIBA, which promotes instability at elevated temperatures.

The chemical transformations at this stage consist of the total decomposition of gel phases, the formation of stable crystalline phases, such as mullite or gehlenite, and the release of gases from sulfate or carbonate decomposition. These processes are contributors to significant structural degradation, and MIBA-rich samples are less durable.

4.2.6. Summary

The colour variations recorded for AAC samples accordingly match the chemical and physical complex processes that can occur during thermal exposure. At room temperature, the samples are dark grey, and the colour becomes increasingly varied and lighter when temperature increases. Dehydration, oxidation, and crystallization bend it towards progression from dark grey to light beige, and the degree of change depends on the percentage of MIBA content.

- **Dehydration** reduces water content and initiates early color changes.
- **Oxidation** of Fe^{2+} to Fe^{3+} intensifies at higher temperatures, producing reddish-brown tones in MIBA-rich samples.
- **Crystallization** forms stable phases like gehlenite, anorthite, and mullite, contributing to lighter tones and reduced durability.

The incorporation of MIBA amplifies these effects, particularly at higher temperatures, where its high CaO and Fe_2O_3 content play a dominant role. Understanding these transformations is essential for optimizing AAC compositions for thermal resistance and durability in high-temperature applications.

M0 at 23℃	M05 at 23℃	M10 at 23℃	M15 at 23℃	M20 at 23℃
M0 at 200℃	M05 at 200℃	M10 at 200℃	M15 at 200℃	M20 at 200℃
M0 at 400℃	M05 at 400℃	M10 at 400℃	M15 at 400℃	M20 at 400℃
M0 at 600℃	M05 at 600℃	M10 at 600℃	M15 at 600℃	M20 at 600℃
M0 at 800℃	M05 at 800℃	M10 at 800℃	M15 at 800℃	M20 at 800℃
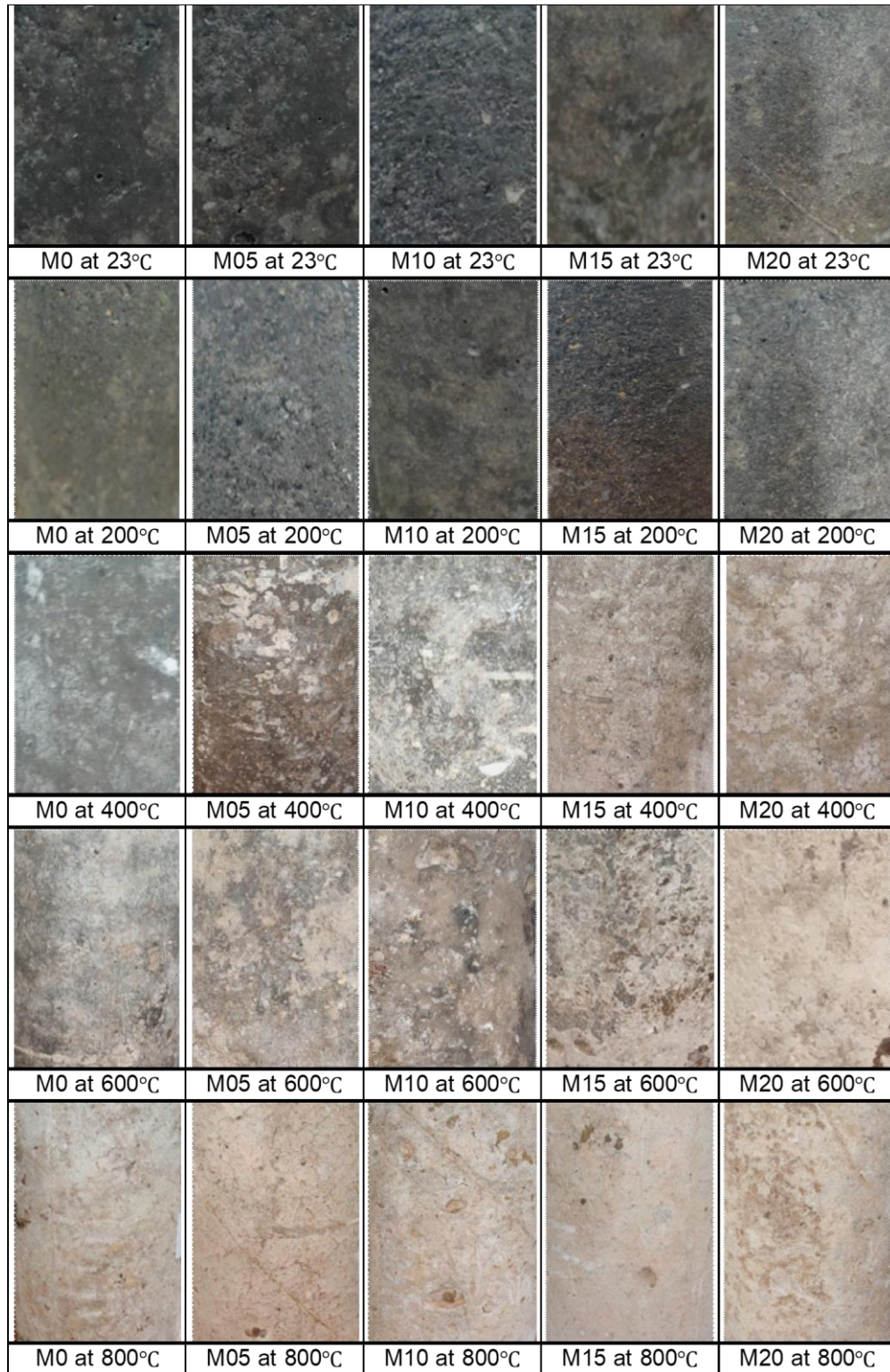
**Figure 4.5: Color variation of AAC due to MIBA content under various elevated temperatures**

4.3. Mass Loss of AAC at Elevated Temperatures

The results indicate that the mass loss of MIBA-AAC at elevated temperatures is mainly due to moisture evaporation, dehydration of binder phases, and thermal decomposition of reaction products, in Figure 4.6. As temperatures rise, this process happens in stages, and the material behaves differently at each stage, with the overall thermal stability differing. The mass loss at temperatures up to 100°C is mainly caused by evaporation of free water in the pore structure of the concrete. Geopolymeric gels start dehydrating the chemically bound water when the temperature is increased to 600 'C, which enhances mass loss, particularly from N-A-S-H and C-S-H phases.

MIBA incorporation alters the thermal behaviour of AAC in that these additional oxides, CaO, Al_2O_3, and SiO_2, impact the geo-polymerization mechanism and stability of the binder phase. At moderate temperatures (100°C–600°C), thermal resistance is enhanced by MIBA, which favours the formation of secondary gel phases to retard gel-ray complexation. However, above 600°C, the decomposition of these gels results in increased porosity and microcracking of the AAC matrix. Mass loss in Figure 4.7(a) also includes the expansion of aggregates and shrinkage of the binder structure.

However, as shown in Figure 4.7(c), the transformation of amorphous geopolymer gels to crystalline phases starts to dominate at 800°C due to pores and void formation. Porosity and degradation of the microstructure are responsible for increased porosity which significantly reduces the material's strength and durability. In addition, CaO from MIBA may even further induce phase transformations and influence the overall thermal stability and resistance to extreme heat of the material.

Although these increased temperatures create more complex structural elements, incorporation of MIBA can improve sustainability through the use of conventional precursors, while achieving acceptable thermal behavior under moderate heat use. However, more attempt is needed to increase thermal resistance to value above 600°C and minimize the mass loss arising from binder thermal degradation. One direction for future research on MIBA-modified AAC is to improve its microstructural integrity to maintain durability and effectiveness in fire resistant construction applications for long term service.
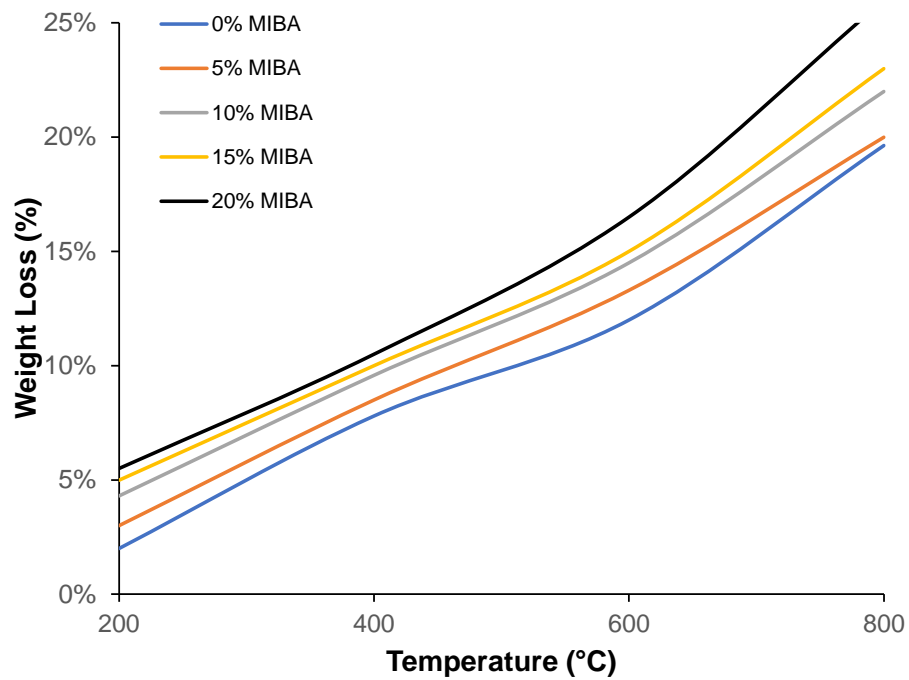
Figure 4.6: Mass Loss behavior of MIBA-AAC at elevated temperatures
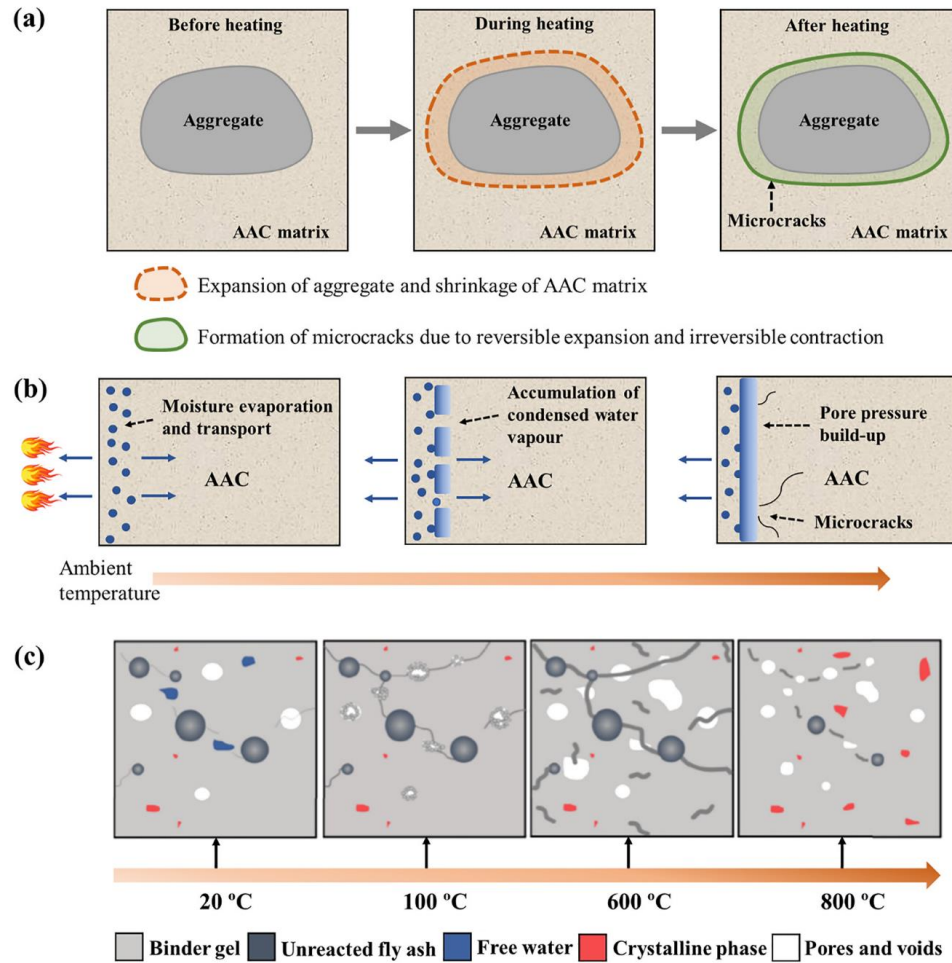
Figure 4.7: Thermal incompatibility (a), pore pressure build-up (b) and phase transformation (c) are the damage mechanisms of AAC at elevated temperatures.

4.4. Heat Transfer Behavior of MIBA-AAC

The analysis of the relation between furnace temperature (the external heat source) and core temperature (the internal heat absorption) provides an assessment of the heat transfer behavior of AAC with MIBA. Figure 4.8 depicts temperature curves of the material for different MIBA replacement levels (M05, M10, M15, and M20) to yield useful heat transfer properties insights. On the contrary, a higher delay between the furnace and the

core temperatures means better thermal resistance, since it means the material's capacity to delay accelerating the heat to penetrate.

4.4.1. Thermal Lag and Heat Transfer Characteristics

A thermal lag is seen on all experimental AAC samples, meaning they decelerate heat transfer. Although the M10 sample exhibits the largest delay between furnace and core temperature, implying the best thermal insulation properties, this sample also offers the least number of cycles before wetout occurs. On the other hand, when the MIBA replacement level surpasses 10% (M15, and M20), core temperature increases at a faster rate implying a decrease in thermal resistance. That means a higher MIBA content raises heat transfer through the material, causing the material to be more readily heated.

4.4.2. Time to Thermal Equilibrium

A second important observation is the time it takes each sample to come to thermal equilibrium. The M05 and M10 samples are slower to stabilize, preventing heat transfer. If not, M15 and M20 reach equilibrium quickly, let heat bypass more easily. This trend further supports MIBA content below the 10% value, as the material's insulating capacity declines with additional MIBA, eliminating the potential for high thermal resistance in such applications.

4.4.3. Implications for Material Optimization

These data demonstrate that the M10 mix is the best compromise between insulation and insulation properties. Above this level, heat transfer increases, making the material less acceptable for applications requiring very high thermal stability. Consequently, the optimal

MIBA replacement level should be chosen with care, given that AAC's structural and thermal performance requirements are those intended. It is suggested that future studies optimize mix design parameters to maximize the insulating efficiency while maintaining mechanical strength and durability.
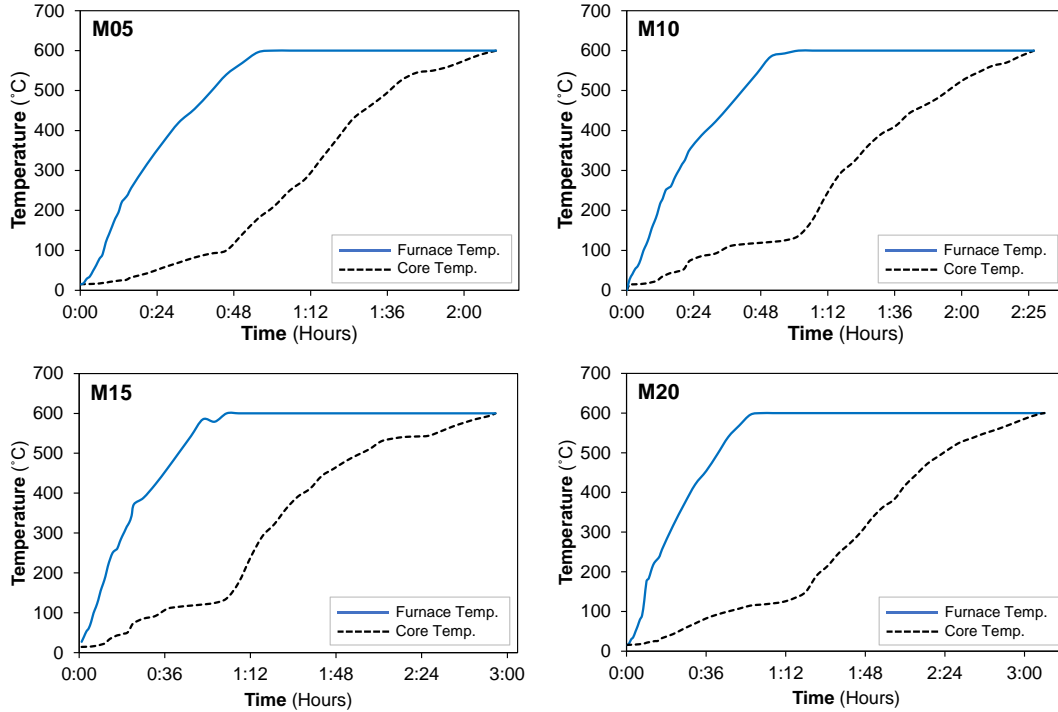
Figure 4.8: Heat transfer behavior of MIBA-AAC

4.5. Impact evaluation of Temperature on AAC through XRD

4.5.1. Impact at 24°C

The XRD patterns of M00 and M20 at room temperature show that crystalline phases such as Quartz (SiO_2) were the most prominent phase with a peak at 26° 2θ, and for M20, MTM was greater than M00. AAC is durable since the formation of quartz is an inert and stable crystalline structure. All samples show another important phase, Mullite ($Al_6Si_2O_{13}$), identified at 32° 2θ. The AAC also incorporates a common phase in fly ash, mullite, a

stable aluminosilicate, which further increases the thermal stability and mechanical properties of the AAC.

In addition, for M10 and M20, an additional peak for Gehlenite ($Ca_2Al_2SiO_7$) appears, especially at 35° 2θ. In addition, it is a high-temperature phase that manifests cementitious behavior. It is reported (Kumar et al., 2018) that gehlenite can promote early-stage strength development in AAC because of its reactivity. There is no significant decomposition or transformation of phases at this stage, indicating material structural stability.

4.5.2. Impact at 400°C

In the temperature range of 400°C some obvious changes in crystalline structure are observed. Mullite ($Al_6Si_2O_{13}$) and Hematite (Fe_2O_3) remain stable ($Q^-s = 1.0$), but new peaks for Hematite appear at 2θ = 35° in M10 and M20, showing that the M5 catalyst is not reducing the Hematite. The iron-containing phases in MIBA and fly ash are considered to be being oxidized. However, this is critical both because the presence of hematite at this temperature contributes to densification of the matrix and improved compressive strength, and also because failure generally occurs through ductile fracture rather than cleavage. M10 and M20 both show the emergence of CSH (Calcium Silicate Hydrate) phases at 50°-55° 2θ. The CSH phases are amorphous to semi-crystalline in nature and largely dominate strength by CSH alone. The effect of MIBA on the CSH peaks is shown to be more pronounced, indicating increased reactivity of the mix with increased MIBA content (M20). It was found that the formation of CSH gels at elevated temperatures densifies the matrix, and improves interfacial bonding (Provis & Bernal, 2014).

4.5.3. Impact at 800°C

The patterns show significant phase transformations at 800°C, with persistent Quartz (SiO_2) as well as Mullite ($Al_6Si_2O_{13}$). The thermal stability of these phases contributes to the durability of AAC, even at high temperatures. Further oxidation processes producing a denser microstructure are indicated by further oxidization of Fe_2O_3 peaks. The stability of quartz and mullite, and residual hematite enhances the thermal resistance and structural integrity of AAC at high temperatures. The intensity of the Gehlenite peak ($Ca_2Al_2SiO_7$) at 35° 2θ increases for M10 and M20, reflecting the contribution of MIBA to high-temperature cementitious reaction. Moreover, the crystallinity of CSH phases increases as indicated in peaks at 50°–55° 2θ. We know this temperature will crystallize the CSH phases to reduce porosity and increase compressive strength (Wang et al., 2021). Strength gains may be offset, however, by excessive crystallization leading to brittleness.

4.5.4. *Impact on Strength Properties*

Crystalline phase transitions observed across temperatures directly affect the strength properties of AAC. Good initial mechanical properties are achieved at room temperature by the inert nature of quartz and its stability as mullite. The reactivity improvement attributable to MIBA is evidenced by the formation of gehlenite as it contributes to early-stage strength. The formation of hematite and semi-crystalline CSH phases densify the matrix, resulting in improvement in compressive strength and thermal stability at 400°C. Stabilization of crystalline phase (e.g., gehlenite, quartz, mullite), enhanced CSH formation & a high heat-resistant matrix comes by 800°C. But when designing AAC materials for high temperature use, there is the potential for brittleness at high temperatures.

These findings are consistent with previous research on AAC such as that reported by Provis and Bernal. A role of CSH phases on strength and durability improvement, notably at elevated temperatures was [15]. Zhang et al. [17] also showed that hematite formation is an important matrix densification mechanism in alkali activated systems. In particular, gehlenite was highlighted as providing significant early-stage strength in systems that contain industrial by products, such as MIBA. Furthermore, Wang et al. (2021) [48] discussed the thermal stability of quartz and mullite in AAC, which agree with the findings of this study. The reported behavior of CSH phase crystallization at higher temperatures is consistent with the literature in the sense that CSH phase can gradually form, leaving an influence on porosity and strength.
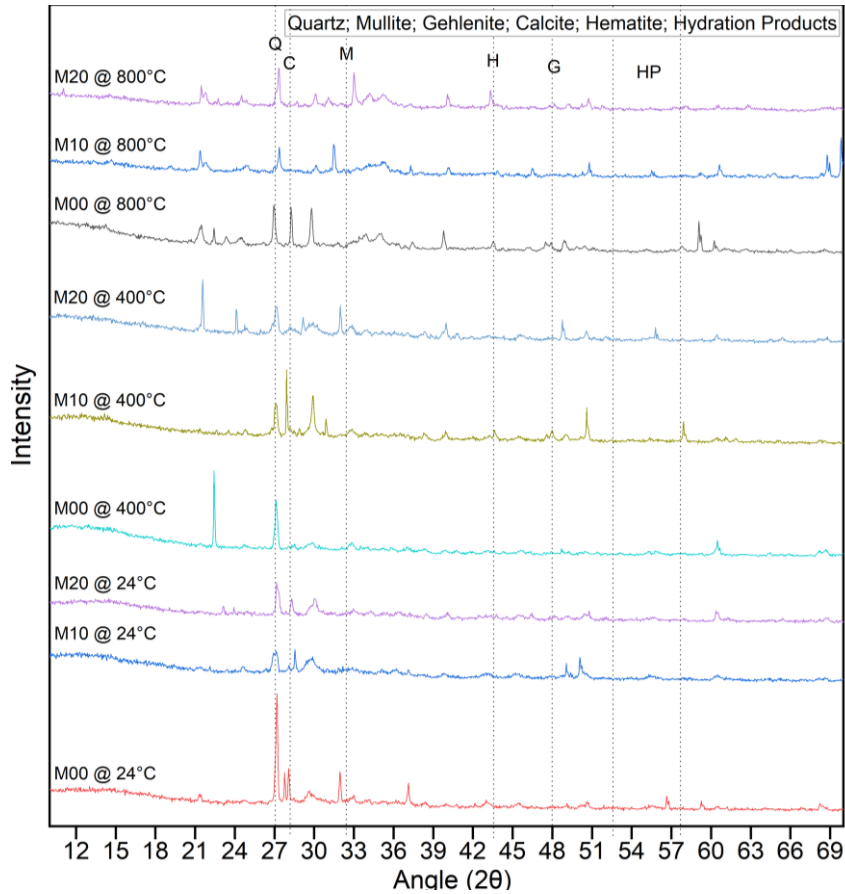
Figure 4.9: XRD patterns for AAC containing MIBA at various temperatures

4.6. Compressive Strength and Mechanical Properties

Test results of Alkali Activated Concrete (AAC) containing various amounts of MIBA show a decreasing compressive strength behavior with increased amount of MIBA inclusion. The highest compressive strength is achieved with the control mix (M00) containing 100% Fly Ash (FA) without MIBA, around 40 MPa, indicating the strong geopolymer gel formation capacity of FA. The stress-strain profile of M00 consists of a sharp peak and sharp decline in stress, suggesting a brittle failure mechanism. This behavior reveals the high strength but limited ductility of the control mix.

4.6.1. Low MIBA Content (M05 and M10)

M05: M05 yields no significant loss of compressive strength compared to M00. The same stress-strain curve is observed with reduced stiffness, represented by a somewhat lower slope in the elastic region. The results indicate that the binding of AAC by small amounts of MIBA does not substantially weaken the binding quality or strength of AAC.

M10: With 10% MIBA, the earlier-mentioned reduction in compressive strength and stiffness shows up with more visibility. Its stress-strain behavior shows a less steep slope and a lower peak stress. MIBA´s reactivity is less than FA, resulting in less workable gel formation and a slightly less dense matrix. However, even though the power density in M10 has fallen, the performance of M10 is still adequate for moderate structural applications.

4.6.2. Moderate to High MIBA Content (M15 and M20)

M15 and M20: The compressive strength declines significantly as the MIBA content rises to 15% and 20%. Stress-strain curves show lower peak stress, flatter elastic slopes, and reduced strain capacity. These mixes demonstrate a brittle failure mode, with minimal deformation before failure, and are characterized by:

- **Reduced binding efficiency:** MIBA's limited ability to form C-S-H and N-A-S-H gels weakens the matrix.

- **Increased porosity:** Higher MIBA content introduces voids, reducing load-bearing capacity.

- **Weaker microstructure:** Microstructural analysis reveals microcracking and poor particle packing, exacerbating early failure under stress.

4.6.3. *Comparative Performance of AAC*

The comparative performance of AAC mixes reveals a clear relationship between MIBA content and compressive strength, as depicted in Figure 10. The control mix (M00) achieves approximately 40 MPa, exhibiting a sharp stress-strain curve that highlights excellent strength but demonstrates brittle behavior. When 5% MIBA (M05) is incorporated, the mix retains adequate stiffness and strength with minimal performance loss. A moderate strength reduction is observed at 10% MIBA (M10), making it suitable for non-critical structural applications. However, mixes with 15% (M15) and 20% (M20) MIBA exhibit significant strength loss and reduced ductility, rendering them unsuitable for load-bearing applications. The compressive strength of AAC tends to go down progressively as MIBA content increases, that is its inverse relationship with matrix quality. For applications that require structural strength, stiffness, and ductility, low MIBA

contents (5–10 %) are sufficient to maintain acceptable mechanical properties, but MIBA contents over 15 % result in large strength, stiffness and ductility losses, limiting their use in structural applications.

By optimizing MIBA content when reaping FA, this analysis also shows the importance of this content. Low levels of MIBA (5–10%) are acceptable for moderate strength applications but proportions above this level severely degrade the structural integrity of the mixes. Furthermore, observational tests reveal that these mixes exhibit an unacceptably high level of brittleness at elevated MIBA level making these mixes unsuitable for applications that require energy absorption or resilience.
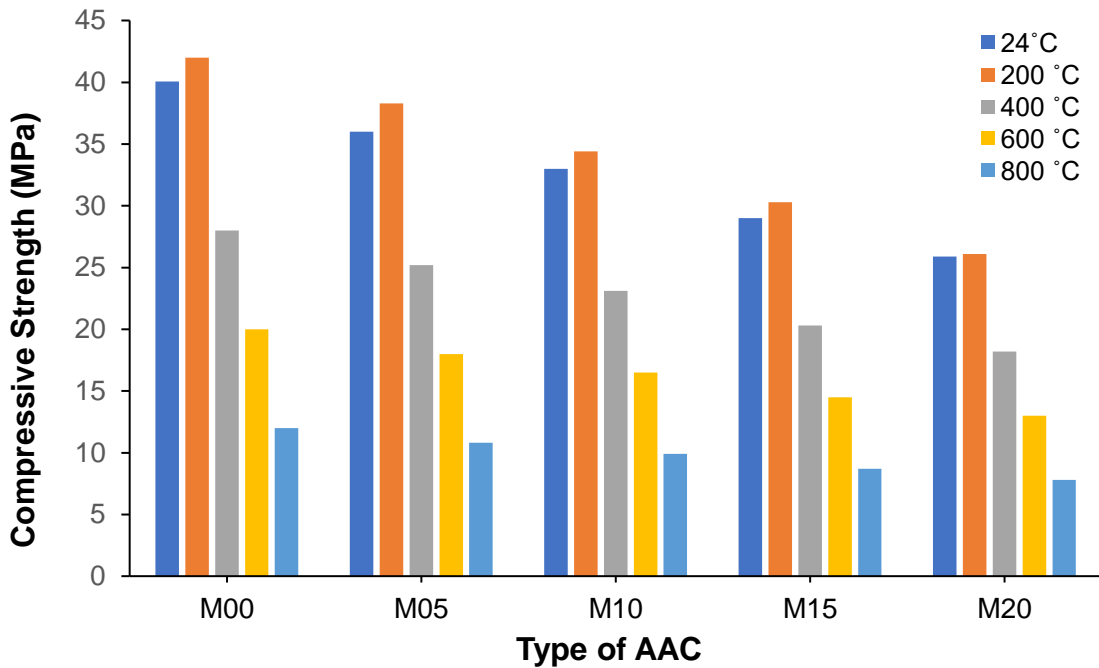
Figure 4.10: Compressive Strength of AAC incorporating MIBA

4.7. Microstructural Analysis of AAC

In Figure 4.11, a SEM analysis of AAC with different levels of MIBA as a partial replacement of FA provides insights on the SEM analysis of AAC into relation with the influence of the microstructure on mechanical and thermal properties. Dense, compact and uniform microstructure with well-formed binding gels such as Calcium Silicate Hydrate (C-S-H), Sodium Alumino Silicate Hydrate (N-A-S-H), and few voids can be seen in the control sample (M00, 0% MIBA). Formation of a strong geopolymer matrix is essential to determination of mechanical and thermal stability, and these gels are important to generating these strong gels. FA and GGBFS were effectively alkali activated to form a robust and durable structure with minimal porosity, little microcracking, and no free unreacted particles.

Conversely, the microstructure differs greatly in the M20 (20% MIBA) sample. M20 exhibits increased porosity, microcracks, and unreacted MIBA particles at ambient temperature (24°C). The lower reactivity of MIBA is confirmed through its reduced formation of reaction products such as C-S-H and N-A-S-H gels. The structure is compromised with rough surface morphology and weaker binding phases realized in the matrix.

The M10 sample presents some binding phases retained at 400°C, with growths of rounded shape that indicate moderate thermal stability. However the matrix develops cracks when it is exposed to thermal stress. However, M20 at 400°C experiences significant cracking, matrix disruptions, and deterioration of C-S-H and N-A-S-H gels. This lack of integrity indicates unreacted particles, which point to MIBA's ability to operate only a few steps

within a chemical reaction before degrading at higher temperatures. At 600°C, M20 deteriorates severely. SEM images reveal widespread porosity, extensive cracking, and the near-total breakdown of binding gels. The primary phases responsible for AAC strength, such as C-S-H and N-A-S-H, decompose, leading to structural collapse. MIBA's inability to form a cohesive geopolymer matrix under thermal stress results in brittle, weak material behavior.

Microstructural degradation is particularly pronounced in high-MIBA samples (M15 and M20), caused by MIBA's lower chemical reactivity. Unlike FA and GGBFS, which contribute significantly to binding phase formation, MIBA introduces heterogeneity and weak points into the matrix. These weak points and increased porosity and cracking compromise structural integrity under ambient and elevated temperature conditions.

The comparison of microstructures highlights the differences across MIBA levels. M00 (0% MIBA) has a dense and well-bonded matrix with minimal defects, providing excellent strength and durability. M10 (10% MIBA) retains moderate binding gels and shows small cracks with slightly higher porosity, maintaining reasonable performance up to 400°C. In contrast, M15 and M20 (15–20% MIBA) exhibit a highly porous structure with significant microcracking, unreacted particles, and weak binding phases, leading to brittle failure and substantial integrity loss, particularly under thermal stress.

The findings demonstrate that MIBA content critically influences AAC's microstructure. While low MIBA levels (≤10%) can maintain a stable and cohesive matrix with acceptable mechanical and thermal performance, higher levels (≥15%) create a porous and poorly

bonded structure, compromising strength and durability. Optimizing MIBA replacement is essential to balance sustainability with performance in AAC.
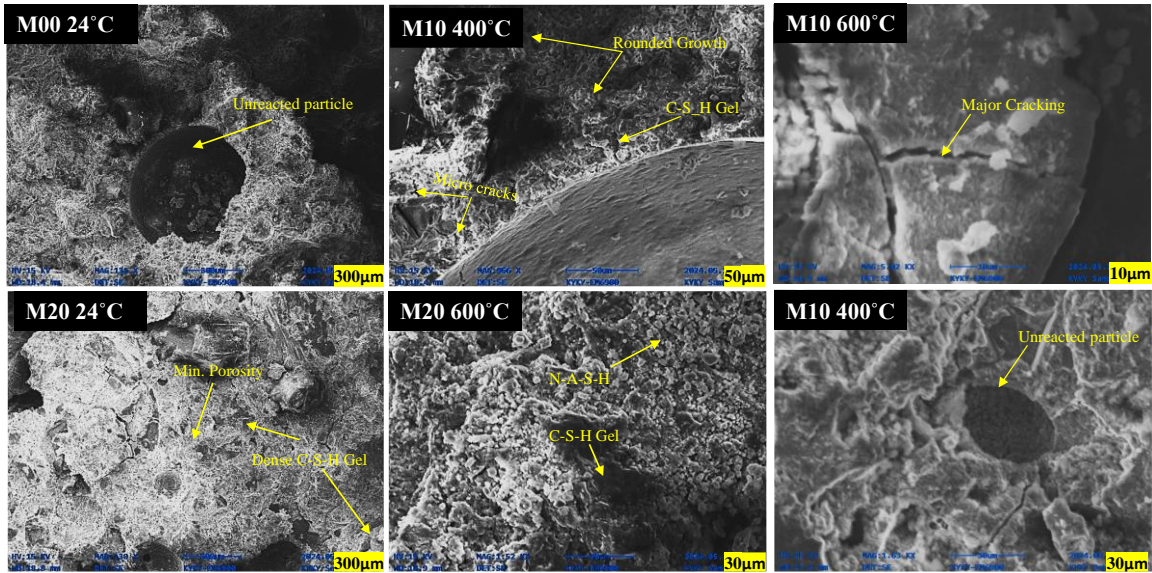
Figure 4.11: SEM images of AAC incorporating MIBA at different levels and exposure conditions

CHAPTER 5: LIFE CYCLE ASSESSMENT

5.1. Introduction and Contextual Framework

The Life Cycle Assessment (LCA) to evaluate AAC incorporating MIBA as a substitute for FA focuses on identifying and quantifying the environmental impacts of various mix formulations. This study underscores the sustainability advantages of utilizing MIBA as an alternative binder material, aligning with circular economy principles by repurposing industrial waste. The LCA adheres to ISO 14040 and 14044 standards, employing a cradle-to-gate approach, with the functional unit defined as "1 m³ of concrete."

The analysis was conducted using OpenLCA software (v2.2.0), leveraging data from the Ecoinvent database and employing the ReCiPe Midpoint 2016 Life Cycle Impact Assessment (LCIA) methodology. This framework enables a comprehensive evaluation of the environmental consequences associated with the production of AAC mixes, providing insights into their potential to reduce ecological impacts through waste material utilization [53,54].

The analytical system boundaries encompass two scenarios for comparison: AAC produced with MIBA (depicted in blue in the process flow diagram) and AAC produced without MIBA (represented in red). These boundaries include all stages from raw material procurement, such as waste collection, drying, and grinding, to the final mixing and casting processes, as illustrated in Figure 5.1. This setup directly evaluates traditional AAC against AAC containing MIBA at substitution levels ranging from 5% to 20%, as detailed in Table 01. The mix design specifications reflect a systematic replacement of FA with MIBA,

maintaining stable quantities of GGBFS, sand, coarse aggregates (CA), and alkali activators (NaOH and Na₂SiO₃). For increasing MIBA content, FA content decreases incrementally to yield a material substitution strategy. Mix design strategy focuses on retaining the structural integrity and workability of concrete and improving its environmental performance without depending on conventional raw materials, as supported sustainability objectives.

5.2. Life Cycle Impact Categories

Environmental impacts relevant for several impact categories including Terrestrial Acidification Potential (TAP), Global Warming Potential (GWP), Terrestrial Ecotoxicity Potential (TETP), Marine Eutrophication Potential (MEP), Ozone Depletion Potential (ODP), and Water Consumption potential (WCP) were evaluated in the LCA. Figures 5.2 and 5.3 show the comparison of the environmental implications of AAC of M00 (zero percent MIBA), through to M20 (20% MIBA).

5.3. Life Cycle Impact Assessment (LCIA)

Increases in MIBA content resulted in large improvements in TAP and MEP. It ranged progressively from 100% in M00 to 85% in M05, 70% in M10, 60% in M15 and 40% in M20. The trend shows how MIBA has the potential to reduce acidifying emissions and lessen the risk of soil acidification. MEP results show a corresponding reduction from 100% in M00 to 85% in M05, 70%, M10, 60% in M15, and 40% in M20, consistent with reduced nutrient pollution that can have positive effects on aquatic habitats that may be suffering eutrophication and algal bloom. The reduced emissions are attributed to the

modified chemical composition of the AAC mixes, where MIBA content is increased at the expense of FA, reducing emissions from acidic and nutrient enriching pollutants.

On the contrary GWP was steadily elevated across all mixes and increased slightly with more MIBA by appearing from 100% in M00 to 103% in M05, 106% in M10, 108% in M15, 110% in M20. The outcome demonstrates that the substitution of FA by MIBA leads to no significant reduction of the carbon footprint of AAC because of the energy intensive nature of the MIBA processing and the use of GGBFS that continues to contribute to an important extent to GWP. As such, these findings suggest that research into energy efficient production methods and the use of renewable energy sources as a means of mitigating the carbon impacts of AAC production is still needed.

TETP and ODP were all very stable and only varied very little across the mixes. However, ODP changed little, while TETP increased slightly from 100% in M00 to 103% in M20. The similar heavy metal and ozone depleting substance concentrations in MIBA and FA are attributed to this stability.

WCP exhibited little or no MIBA substitution reduction either. Pursuing optimal water management approaches to boosting the sustainability of AAC is more critical in regions affected by water scarcity as the water demand for mixing and curing stays the same irrespective of the formulation.

The further elaboration on the contributions of individual ingredients (GGBFS, FA, sand, gravel, NaOH, and MIBA) to environmental impact categories in Figure 5.4. GWP and TETP were identified to be dominated by GGBFS and FA, which had significant environmental burdens. Though shifting MIBA for FA altered the distribution of impacts,

76

MIBA's contribution to total impacts decreased slightly and accordingly, both MIBA's environmental inputs and its associated energy requirements increased slightly. Those additional processing steps for MIBA, incineration, magnetic separation and ball milling, highlight the complexity of the production process and in turn the impacts from the additional processing steps.

5.4. Challenges and Recommendations

Despite TAP and MEP reductions are promising, the environmental profile of AAC with MIBA substitution lags because of high GWP and persistent water consumption. The energy intensive nature of the processes used in MIBA preparation magnifies their impacts on the GWP, emphasizing the importance of the optimization of these processes in order to enhance the environmental performance of AAC. Future research should integrate renewable energy sources, develop energy efficient processing techniques, and maximize the sustainability of AAC through the mix design, by maximizing energy efficiency of processing and the renewable energy used in production. Long-term durability studies of AAC with higher MIBA Content are also needed to ensure the mechanical and environmental performance of the AAC meets the sustainability objectives of the construction sector.

Table 5.1: Impact categories for LCA

Impact Categories	Units
Terrestrial acidification potential (TAP)	kg SO_2-Eq
Global warming potential (climate change) (GWP1000)	kg CO_2-Eq
Terrestrial ecotoxicity potential (TETP)	kg 1,4-DCB-Eq
Freshwater eutrophication potential (FEP)	kg P-Eq
Marine eutrophication potential (MEP)	kg N-Eq
Human toxicity potential (carcinogenic) (HTPc)	kg 1,4-DCB-Eq
Human toxicity potential (non-carcinogenic) (HTPnc)	kg 1,4-DCB-Eq
Ozone depletion potential (ODP)	kg CFC-11-Eq
Water consumption potential (WCP)	m^3
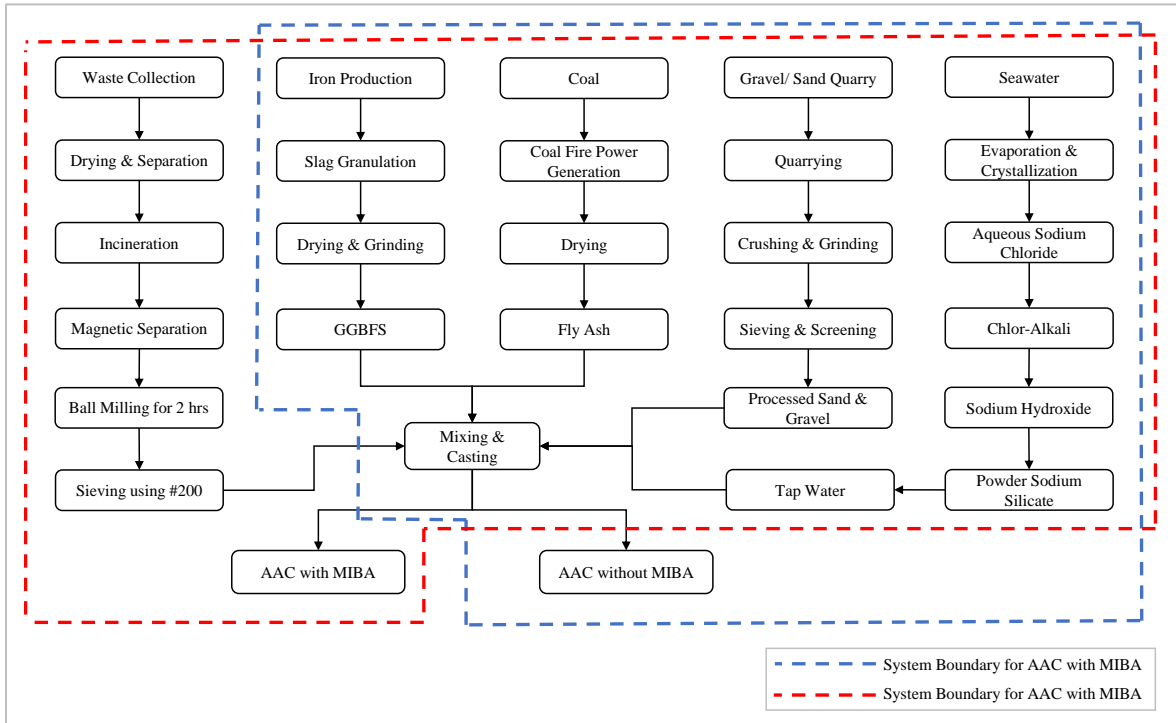
Figure 5.1: Cradle-to-gate system boundary for AAC with & without MIBA
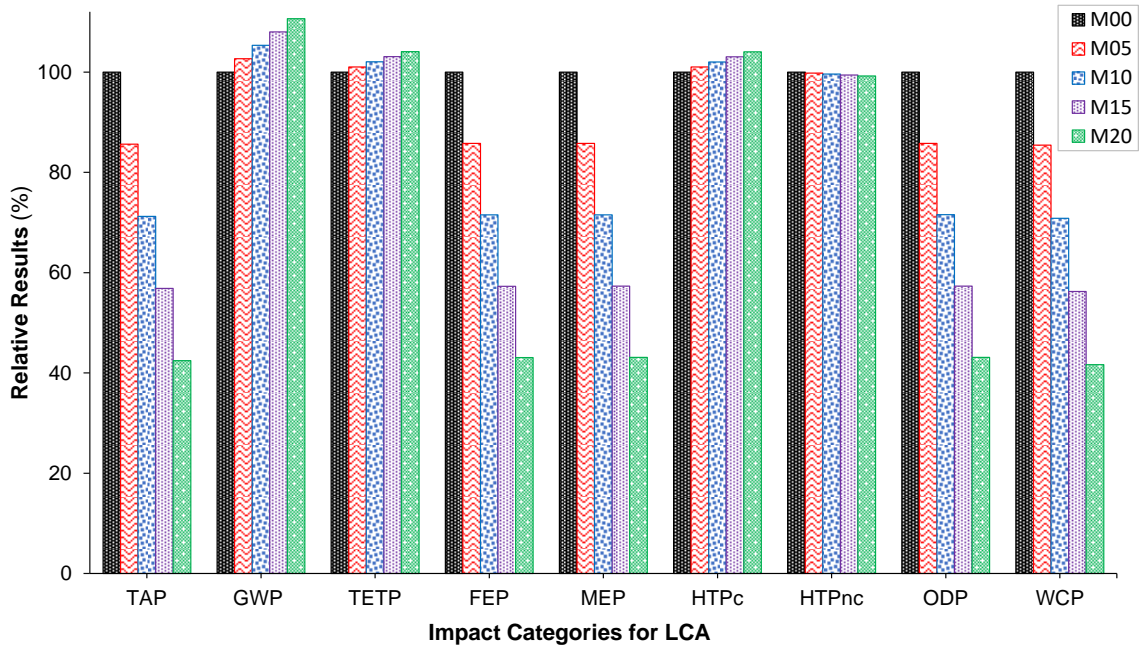
Figure 5.2: Relative results of impact categories for AAC
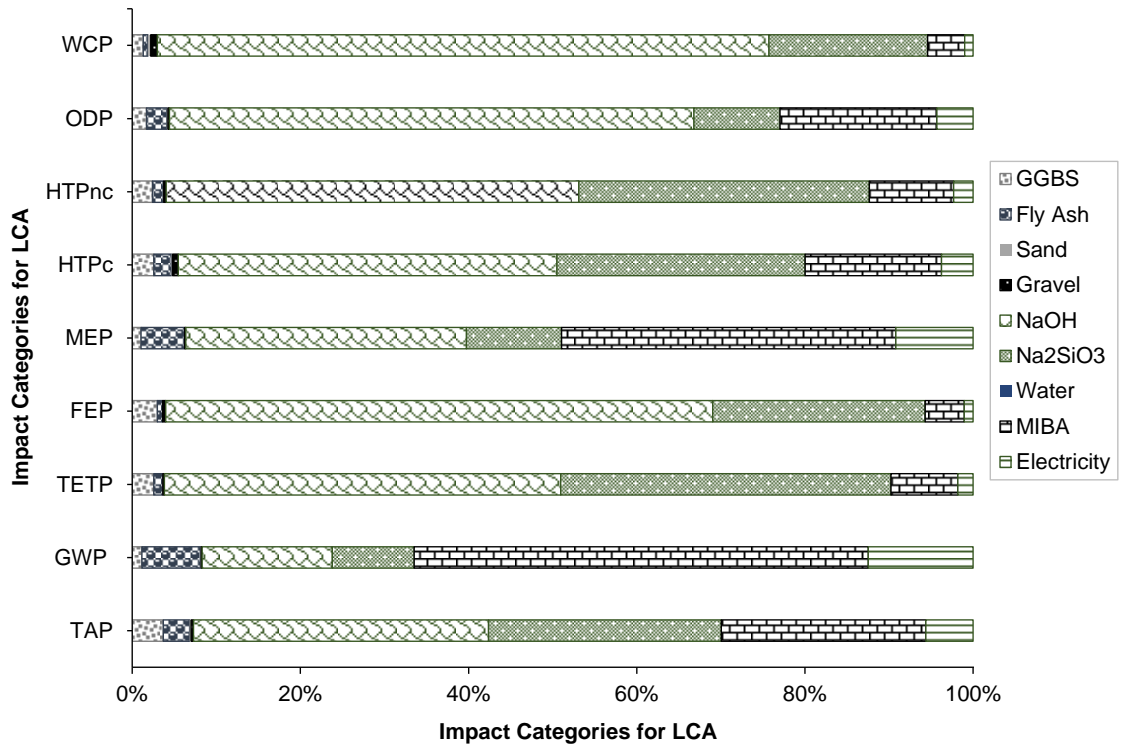

Figure 5.3: Role of Each Ingredient of Mix on Impact Categories

CONCLUSIONS

This study evaluated at elevated temperatures the performance of Alkali Activated Concrete (AAC), partially replaced with Municipal Waste Incinerator Bottom Ash (MIBA), as a partial replacement for Fly Ash (FA). The research thus explores the effects of mechanical behavior, thermal stability, phase transformations and environmental sustainability through experimental investigations, life cycle analysis (LCA), and microstructural analysis.

- The MIBA characterization revealed to be a potential precursor replacement for the Alkali activated concrete. It has similar compounds, FA and GGBFS, but at different levels. However extensive preprocessing must be required for the replacement in large quantities.

- Results show that the most plentiful replacement of MIBA contained 10% (M10 mix). In terms of compressive strength, durability and thermal resistance. Increasing MIBA content (>15%) resulted in increasing porosity, and this increased the rate of microcracking, ultimately limiting overall mechanical integrity. The M10 mix exhibited effectively delaying heat penetration, and thermal degradation was significant beyond 600°C in AAC samples. reaction product decomposition.

- SEM and XRD microstructural analysis confirmed changes to the MIBA. The alkali activation, and its effect on gel formation and binder stability. At moderate MIBA was found to contribute to denser reaction products at higher compromised

by temperatures, phase transformations and increased porosity mechanical performance.

- From an environmental perspective, implementing MIBA into AAC resulted in notable sustainability benefits. The LCA results showed a 60% reduction in Terrestrial Acidification Potential (TAP) and Marine Eutrophication Potential (MEP), indicating that MIBA significantly lowers environmental impacts related to resource depletion. However, Global Warming Potential (GWP) remained stable, suggesting that energy-efficient MIBA processing methods are crucial for reducing carbon emissions.

Overall, MIBA-incorporated AAC is a promising, sustainable material with potential applications in fire-resistant construction. However, further refinements are needed to optimize durability, workability, and large-scale feasibility.

FURTURE RESEARCH RECOMMENDATION(S)

To further optimize MIBA in AAC, the following key research directions are recommended:

1. Investigate higher MIBA replacement levels (>20%) with complementary materials like silica fume, metakaolin, or rice husk ash to enhance strength and thermal performance.

2. Assess carbonation resistance, freeze-thaw cycles, sulfate attack, and chloride penetration to ensure structural stability in harsh environments. Study heavy metal leaching under different conditions for environmental safety.

3. Improve MIBA processing methods for greater sustainability and treatment of MIBA for improved reactivity in the AAC mix.

REFERENCES

1. Yang, K.H.; Song, J.K.; Song, K. Il Assessment of CO 2 Reduction of Alkali-Activated Concrete. *J. Clean. Prod.* **2013**, *39*, 265–272, doi:10.1016/j.jclepro.2012.08.001.

2. Abbass, M.; Singh, G. Microstructural Analysis of Environment Friendly Sustainable Geopolymer Concrete. *Multiscale Multidiscip. Model. Exp. Des.* **2024**, *7*, 301–319, doi:10.1007/s41939-023-00200-w.

3. Amran, M.; Debbarma, S.; Ozbakkaloglu, T. Fly Ash-Based Eco-Friendly Geopolymer Concrete: A Critical Review of the Long-Term Durability Properties. *Constr. Build. Mater.* **2021**, *270*, 121857, doi:10.1016/j.conbuildmat.2020.121857.

4. Zhu, W.; Teoh, P.J.; Liu, Y.; Chen, Z.; Yang, E.H. Strategic Utilization of Municipal Solid Waste Incineration Bottom Ash for the Synthesis of Lightweight Aerated Alkali-Activated Materials. *J. Clean. Prod.* **2019**, *235*, 603–612, doi:10.1016/j.jclepro.2019.06.286.

5. Palomo, A.; Grutzeck, M.W.; Blanco, M.T. Alkali-Activated Fly Ashes: A Cement for the Future. *Cem. Concr. Res.* **1999**, *29*, 1323–1329, doi:10.1016/S0008-8846(98)00243-9.

6. Provis, J.L.; Van Deventer, J.S.J. *Alkali Activated Materials: State-of-the-Art Report, RILEM TC 224-AAM*; Springer Science & Business Media, 2014; Vol. 13; ISBN 9400776713.

7. Abbass, M.; Singh, G. Experimental Investigation of Alkali-Activated Hybrid Geopolymer Concrete. *Multiscale Multidiscip. Model. Exp. Des.* **2023**, *6*, 235–249, doi:10.1007/s41939-023-00144-1.

8. Ozturk, M.; Bankir, M.B.; Bolukbasi, O.S.; Sevim, U.K. Alkali Activation of Electric Arc Furnace Slag: Mechanical Properties and Micro Analyzes. *J. Build. Eng.* **2019**, *21*, 97–105, doi:10.1016/j.jobe.2018.10.005.

9. Rowlatt, J. Coal: Is This the Beginning of the End? Available online: https://www.bbc.com/news/science-environment-50520962 (accessed on 30 June 2024).

10. Margallo, M.; Taddei, M.B.M.; Hernández-Pellón, A.; Aldaco, R.; Irabien, Á. Environmental Sustainability Assessment of the Management of Municipal Solid Waste Incineration Residues: A Review of the Current Situation. *Clean Technol. Environ. Policy* **2015**, *17*, 1333–1353, doi:10.1007/s10098-015-0961-6.

11. Avila, Y.; Vasco, R.S.; Brito, J. De Alkali-Activated Materials with Pre-Treated Municipal Solid Bottom Ash. **2022**.

12. Kumar, V.; Kumar, P. Self-Compacted Geopolymer Concrete Incorporating Waste Ceramic Powder. *Multiscale Multidiscip. Model. Exp. Des.* **2024**, doi:10.1007/s41939-024-00510-7.

13. Kuroki, R.; Ohya, H.; Ishida, K.; Yamazaki, K. Development of Metal Recovery Process for Municipal Incineration (MIBA). *J. Korean Inst, Resour. Recycl.* **2019**, *28*, 21–25, doi:https://doi.org/10.7844/kirr.2019.28.3.21.

14. Lynn, C.J. Municipal Incinerated Bottom Ash Use as a Cement Component in Concrete Municipal Incinerated Bottom Ash Use as a Cement Component in Concrete. **2024**, doi:10.1680/jmacr.16.00432.

15. Provis, J.L.; Bernal, S.A. Geopolymers and Related Alkali-Activated Materials. *Annu. Rev. Mater. Res.* **2014**, *44*, 299–327, doi:10.1146/annurev-matsci-070813-113515.

16. Zhang, Z.; Yang, T.; Wang, H. *Alkali-Activated Cement (AAC) From Fly Ash and High-Magnesium Nickel Slag*; Elsevier Inc., 2017; ISBN 9780128045404.

17. Wang, D.; Luo, B.; Deng, J.; Feng, Q.; Zhang, W.; Deng, C.; Mensah, R.A.; Restas, A.; Racz, S.; Rauscher, J.; et al. Optimized Fire Resistance of Alkali-Activated High-Performance Concrete by Steel Fiber. *J. Therm. Anal. Calorim.* **2024**, doi:10.1007/s10973-024-13238-w.

18. Pacheco-Torgal, F.; Labrincha, J.A. The Future of Construction Materials Research and the Seventh Un Millennium Development Goal: A Few Insights. *Constr. Build. Mater.* **2013**, *40*, 729–737, doi:10.1016/j.conbuildmat.2012.11.007.

19. Siddique, R. Utilization of Municipal Solid Waste (MSW) Ash in Cement and Mortar. *Resour. Conserv. Recycl.* **2010**, *54*, 1037–1047, doi:10.1016/j.resconrec.2010.05.002.

20. Chen, W.; Brouwers, H.J.H. The Hydration of Slag, Part 1: Reaction Models for Alkali-Activated Slag. *J. Mater. Sci.* **2007**, *42*, 428–443, doi:10.1007/s10853-006-0873-2.

21. Bernal, S.A.; Provis, J.L. Durability of Alkali-Activated Materials: Progress and Perspectives. *J. Am. Ceram. Soc.* **2014**, *97*, 997–1008, doi:10.1111/jace.12831.

22. Li, J. Municipal Solid Waste Incineration Ash-Incorporated Concrete: One Step towards Environmental Justice. *Buildings* **2021**, *11*, doi:10.3390/buildings11110495.

23. Pan, Z.; Sanjayan, J.G. Stress-Strain Behaviour and Abrupt Loss of Stiffness of Geopolymer at Elevated Temperatures. *Cem. Concr. Compos.* **2010**, *32*, 657–664, doi:10.1016/j.cemconcomp.2010.07.010.

24. Provis, J.L. Alkali-Activated Materials. *Cem. Concr. Res.* **2018**, *114*, 40–48,

doi:10.1016/j.cemconres.2017.02.009.

25. Bernal, S.A.; Rodríguez, E.D.; De Gutiérrez, R.M.; Provis, J.L. Performance at High Temperature of Alkali-Activated Slag Pastes Produced with Silica Fume and Rice Husk Ash Based Activators. *Mater. Constr.* **2015**, *65*, doi:10.3989/mc.2015.03114.

26. Nath, P.; Sarker, P.K. Effect of GGBFS on Setting, Workability and Early Strength Properties of Fly Ash Geopolymer Concrete Cured in Ambient Condition. *Constr. Build. Mater.* **2014**, *66*, 163–171, doi:10.1016/j.conbuildmat.2014.05.080.

27. Poon, C.S.; Lam, L.; Wong, Y.L. Study on High Strength Concrete Prepared with Large Volumes of Low Calcium Fly Ash. *Cem. Concr. Res.* **2000**, *30*, 447–455, doi:10.1016/S0008-8846(99)00271-9.

28. Criado, M.; Fernández-Jiménez, A.; Palomo, A. Alkali Activation of Fly Ash: Effect of the SiO2/Na2O Ratio. Part I: FTIR Study. *Microporous Mesoporous Mater.* **2007**, *106*, 180–191, doi:10.1016/j.micromeso.2007.02.055.

29. Woo, B.H.; Jeon, I.K.; Yoo, D.H.; Kim, S.S.; Lee, J.B.; Kim, H.G. Utilization of Municipal Solid Waste Incineration Bottom Ash as Fine Aggregate of Cement Mortars. *Sustain.* **2021**, *13*, doi:10.3390/su13168832.

30. Shi, D.; Ren, D.; Ma, Z. Impact of Municipal Solid Waste Incineration Bottom Ash as Cement Substitution. *Arab. J. Sci. Eng.* **2024**, doi:10.1007/s13369-024-09542-0.

31. Gowda, S.; Kunjar, V.; Gupta, A.; Havanagi, V.G.; Kavitha, G. Municipal Incinerated Solid Waste Bottom Ash as Sustainable Construction Material in the Construction of Flexible Pavements. *J. Mater. Cycles Waste Manag.* **2023**, *25*, 3824–3833, doi:10.1007/s10163-023-01809-2.

32. Abubakr, A.; Soliman, A. Impact Behaviour of Steel-Fibre-Reinforced Alkali-Activated Slag Concrete Exposed to Elevated Temperatures. *Materials (Basel).* **2023**, *16*, doi:10.3390/ma16114096.

33. Ramagiri, K.K.; Maeijer, P.K. De Assessment of Alkali-Activated Concrete (AAC). **2022**.

34. Lin, D.F.; Lin, K.L.; Wang, W.J.; Yang, A.C. Blending Electric Arc Furnace Slag and Municipal Incineration Bottom Ash to Make Ceramic Tiles. *J. Mater. Cycles Waste Manag.* **2024**, *26*, 1527–1543, doi:10.1007/s10163-024-01906-w.

35. Lamaa, G.; Duarte, A.P.C.; Silva, R.V.; de Brito, J. Carbonation of Alkali-Activated Materials: A Review. *Materials (Basel).* **2023**, *16*, doi:10.3390/ma16083086.

36. Anburuvel, A. The Role of Activators in Geopolymer-Based Stabilization for Road Construction: A State-of-the-Art Review. *Multiscale Multidiscip. Model. Exp. Des.* 2023, *6*, 41–59.

37. Tupayachy-Quispe, D.; Almirón, J.; Apaza, F.; Churata, R.; Torres-carrasco, M.; Bautista, A. Peruvian Volcanic Ashes as New Alternative Material in Geopolymer Preparation : Influence of Dissolution Concentration and Wear Resistance. In Proceedings of the 8th LACCEI International Multi-Conference for Engineering, Education, and Technology; 2020; pp. 27–31.

38. Ulloa, N.; Onyelowe, K.C.; Ebid, A.M.; Curay Yaulema, C.S.; Zuiga Rodguez, M.G.; Adrade Vally, A.I.; Onyia, M.E. Influence of Alkali Molarity on Compressive Strength of High-Strength Geopolymer Concrete Using Machine Learning Techniques Based on Curing Regimes and Temperature. *Front. Built Environ.* **2024**, *10*, 1–19, doi:10.3389/fbuil.2024.1455915.

39. Casanova, S.; Silva, R. V.; de Brito, J.; Pereira, M.F.C. Mortars with Alkali-Activated Municipal Solid Waste Incinerator Bottom Ash and Fine Recycled Aggregates. *J. Clean. Prod.* **2020**, *289*, 125707, doi:10.1016/j.jclepro.2020.125707.

40. Carvalho, R.; Silva, R. V.; de Brito, J.; Pereira, M.F.C. Alkali Activation of Bottom Ash from Municipal Solid Waste Incineration: Optimization of NaOH- and Na 2SiO3-Based Activators. *J. Clean. Prod.* **2021**, *291*, 125930, doi:10.1016/j.jclepro.2021.125930.

41. Huang, G.; Yang, K.; Sun, Y.; Lu, Z.; Zhang, X.; Zuo, L.; Feng, Y.; Qian, R.; Qi, Y.; Ji, Y.; et al. Influence of NaOH Content on the Alkali Conversion Mechanism in MSWI Bottom Ash Alkali-Activated Mortars. *Constr. Build. Mater.* **2020**, *248*, 118582, doi:10.1016/j.conbuildmat.2020.118582.

42. Xuan, D.; Tang, P.; Poon, C.S. MSWIBA-Based Cellular Alkali-Activated Concrete Incorporating Waste Glass Powder. *Cem. Concr. Compos.* **2019**, *95*, 128–136, doi:10.1016/j.cemconcomp.2018.10.018.

43. Liu, Y.; Sidhu, K.S.; Chen, Z.; Yang, E.H. Alkali-Treated Incineration Bottom Ash as Supplementary Cementitious Materials. *Constr. Build. Mater.* **2018**, *179*, 371–378, doi:10.1016/j.conbuildmat.2018.05.231.

44. Cristelo, N.; Segadães, L.; Coelho, J.; Chaves, B.; Sousa, N.R.; de Lurdes Lopes, M. Recycling Municipal Solid Waste Incineration Slag and Fly Ash as Precursors in Low-Range Alkaline Cements. *Waste Manag.* **2020**, *104*, 60–73, doi:10.1016/j.wasman.2020.01.013.

45. Zhang, B.; Ma, Y.; Yang, Y.; Zheng, D.; Wang, Y.; Ji, T. Improving the High Temperature Resistance of Alkali-Activated Slag Paste Using Municipal Solid Waste Incineration Bottom Ash. *J. Build. Eng.* **2023**, *72*, doi:10.1016/j.jobe.2023.106664.

46. Chen, B.; Perumal, P.; Illikainen, M.; Ye, G. A Review on the Utilization of Municipal Solid Waste Incineration (MSWI) Bottom Ash as a Mineral Resource for Construction Materials. *J. Build. Eng.* **2023**, *71*, 106386, doi:10.1016/j.jobe.2023.106386.

47. Sun, B.; Sun, Y.; Ye, G.; De Schutter, G. A Mix Design Methodology of Blast Furnace Slag and Fly Ash-Based Alkali-Activated Concrete. *Cem. Concr. Compos.* **2023**, *140*, 105076, doi:10.1016/j.cemconcomp.2023.105076.

48. Lian, C.; Wang, Y.; Liu, S.; Hao, H.; Hao, Y. Experimental Study on Dynamic Mechanical Properties of Fly Ash and Slag Based Alkali-Activated Concrete. *Constr. Build. Mater.* **2023**, *364*, 129912, doi:10.1016/j.conbuildmat.2022.129912.

49. Suescum-Morales, D.; Silva, R.V.; Bravo, M.; Jiménez, J.R.; Fernández-Rodríguez, J.M.; de Brito, J. Effect of Incorporating Municipal Solid Waste Incinerated Bottom Ash in Alkali-Activated Fly Ash Concrete Subjected to Accelerated CO2 Curing. *J. Clean. Prod.* **2022**, *370*, doi:10.1016/j.jclepro.2022.133533.

50. Giro-Paloma, J.; Mañosa, J.; Maldonado-Alameda, A.; Quina, M.J.; Chimenos, J.M. Rapid Sintering of Weathered Municipal Solid Waste Incinerator Bottom Ash and Rice Husk for Lightweight Aggregate Manufacturing and Product Properties. *J. Clean. Prod.* **2019**, *232*, 713–721, doi:10.1016/j.jclepro.2019.06.010.

51. Li, X.G.; Liu, Z.L.; Lv, Y.; Cai, L.X.; Jiang, D.B.; Jiang, W.G.; Jian, S. Utilization of Municipal Solid Waste Incineration Bottom Ash in Autoclaved Aerated Concrete. *Constr. Build. Mater.* **2018**, *178*, 175–182, doi:10.1016/j.conbuildmat.2018.05.147.

52. Ghouleh, Z.; Shao, Y. Turning Municipal Solid Waste Incineration into a Cleaner Cement Production. *J. Clean. Prod.* **2018**, *195*, 268–279, doi:10.1016/j.jclepro.2018.05.209.

53. Van Den Heede, P.; De Belie, N. Environmental Impact and Life Cycle Assessment (LCA) of Traditional and "green" Concretes: Literature Review and Theoretical Calculations. *Cem. Concr. Compos.* **2012**, *34*, 431–442, doi:10.1016/j.cemconcomp.2012.01.004.

54. Nikravan, M.; Firdous, R.; Stephan, D. Life Cycle Assessment of Alkali-Activated Materials: A Systematic Literature Review. *Low-carbon Mater. Green Constr.* **2023**, *1*, 1–24, doi:10.1007/s44242-023-00014-6.